



# Benchmark tests for separating $n$ time components of runoff with one stable isotope tracer

Simon Hoeg<sup>1</sup>

<sup>1</sup>Water Research Agency, D-69257 Wiesbaden, Germany

**Correspondence:** Simon Hoeg (simon.hoeg@waterresearch.eu)

**Abstract.** A validation of the recently introduced iterative extension of the standard two-component hydrograph separation method is presented. The data for testing this method are retrieved from a random rainfall generator and a rainfall-runoff model composed of linear reservoirs. The results show that it is possible to reconstruct the simulated event water response of a given random model input by applying the iterative separation model and using a single stable isotope tracer. The benchmark model also covers the partially delayed response of event water so that a situation can be simulated in which pre-event water is rapidly mobilized. It is demonstrated how mathematical constraints, such as an ill-conditioned linear equation system, may influence the separation of the event water response. In addition, it is discussed how the volume weighted separated event water response can serve as an estimator for a time-varying backward travel time distribution.

## 1 Introduction

Over the past few decades, the separation of storm hydrographs using stable isotope tracers has become a standard method for investigating runoff generation processes in catchment hydrology. It is an approach that relies on steady-state mass balance equations, whereby the early pioneering work was accomplished in the late 1960s and 1970s (Pinder and Jones (1969), Dincer et al. (1970), Martinec et al. (1974), and Fritz et al. (1976), Sklash and Farvolden (1979)), over the years, the methodology has been progressively expanded and adapted to the given challenges and tasks in the field. On the catchment scale, for instance, stable isotope tracers (deuterium, oxygen-18, or tritium) have been combined with geochemical tracers, such as electric conductivity and various cations and anions (Hooper and Shoemaker (1986), Kennedy et al. (1986), Obradovic and Sklash (1986), Matsubayashi et al. (1993), dissolved silica (Maulé and Stein (1990), Hinton et al. (1994), Hoeg et al. (2000)) and dissolved organic carbon (Brown et al. (1999), Ladouche et al. (2001)) to more exactly determine the source areas of runoff and flow pathways. Systematic approaches have been introduced to identify suitable end-members (Christophersen et al. (1990), Christophersen and Hooper (1992), Hooper (2003), Barthold et al. (2011) Delsman et al. (2013)) and to estimate the uncertainty of separated components (Genereux (1998), Joerin et al. (2002) Uhlenbrook and Hoeg (2003)). Furthermore, balance equations have been connected to displacement mechanisms by an ordinary differential (Laudon et al. (2002)) or travel time distributions (Weiler et al. (2003), Lyon et al. (2008), Segura et al. (2012)), hence involving the travel times of event water within the catchment. In addition, a stochastic framework has been established, linking time-varying residence, travel, and evapotranspiration time distributions in terms of the relevant input or output fluxes and of the type of mixing taking place



in the catchment transport volumes ((Botter et al. (2011)), Harman (2015)). The age-ranked hydrological budgets and travel time descriptions have been reworked from the point of view of the hydrological storages and fluxes involved (Rigon et al. (2016)). Furthermore, recently, there has been some progress. For instance, Kirchner (2019) used regressions between tracer fluctuations in precipitation and discharge to estimate the average fraction of new water in a streamflow across an ensemble of time steps. Von Freyberg et al. (2018) expressed event- and pre-event water volumes as fractions of precipitation rather than discharge, which was helpful for investigating the catchments' hydrological behavior. Kirchner and Allen (2020) further emphasized this perspective by showing a seasonal partitioning of precipitation between streamflow and evapotranspiration.

Basically, physical assumptions and knowledge can be included directly in the balance equation structure. For instance, the pre-event water component itself can be subject to the mass conservation of the tracer and volume flow regarding the next prior rainfall-runoff event. Hoeg (2019) recently considered this assumption and proposed a method that iteratively extends the standard two-component separation, such that  $n$  time components are separated by using a single stable isotope tracer. This new approach can be used to trace the event water over a much longer period after the initial event, hence expanding the space of addressable use cases for catchment hydrologists. Hoeg (2019) applied the new method to an experimental data set of the mountainous Zastler catchment (18.4 km<sup>2</sup>, southern Black Forest, Germany) and compared the outcome with previous investigations in that area, showing the influence of antecedent moisture conditions on the event water contributions of subsequent events. The iterative extension was able to uncover the temporal structure of the pre-event component, enabling a closer look at the temporal composition of the pre-event water, hence determining the extent to which recent events are involved.

Comparative reviews published over the last years (Buttle (1994), Klaus and McDonnell (2013)) have shown the enormous range and abundance of field studies that have taken advantage of isotope tracer observations and mass balance-based hydrograph separations. Recently, Jasechko (2019) reviewed over 100 studies that have applied isotope compositions to calculate the fractions of streamflow comprising of pre-event water. Jasechko (2019) reported that among the  $n=101$  compiled studies, the majority ( $n=61$ ) reported that more than half of the streamflow is comprised of groundwater (i.e., minimum pre-event water fraction exceeding 50%). Most studies ( $n=86$ ) have calculated that groundwater may comprise more than half of the streamflow (i.e., maximum pre-event water fraction exceeding 50%). It has been shown in many studies that the specific behavior of the event and pre-event component can be related to the postulated runoff generation processes on site (Sklash and Farvolden (1979), Maulé and Stein (1990), Ogunkoya and Jenkins (1993), Hoeg et al. (2000), Weiler et al. (2003), Iorgulescu et al. (2007), James and Roulet (2009), Segura et al. (2012)) that are subject to complex physical dynamics (Freeze (1974), Kirkby (1979), Buttle (1998), Bonell (1998)).

For catchment hydrologists it is important to have knowledge of the reliability of the methods that assist in analyzing runoff generation processes. Every systematic error analysis will assist in putting the statements made into perspective. The current study contributes here in three aspects:

1. A validation of the iterative approach suggested by Hoeg (2019) is shown based on a linear rainfall-runoff model and synthetic-generated precipitation data. The aim (benchmark) is the reconstruction of the simulated event water response of a given model input. Here, different scenarios are considered, in which the iterative separation model also reveals its limits. It is expected that the tests will help to evaluate and understand the skills of the iterative hydrograph separation. For



the recently introduced ensemble hydrograph separation approach, through benchmark testing Kirchner (2019) assessed how accurate the applied method is, and what factors might affect its accuracy.

2. A measure (the condition number) is introduced that describes how strongly an input error can affect the calculated output in the worst case. This helps to evaluate the mathematical constraints that arise directly from the applied separation model. Therefore, the condition number is the appropriate measure to support the intention of the current work to obtain a sense of the reliability of the method.
3. A consideration of how the results of the iterative separation approach can be related to the description of travel times in catchment hydrology, which is expected to be one of the favorite applications, but has not been analyzed in detail yet.

## 2 Methods

### 2.1 Separation of $n$ time components

Consider a control volume, for instance, a catchment in a river basin, with the following bulk water balance:

$$\frac{dS(t)}{dt} = J(t) - ET(t) - Q_t(t) \quad (1)$$

where  $S(t)$  is the time evolution of the water storage,  $J(t)$  is the precipitation,  $ET(t)$  is the evapotranspiration, and  $Q_t(t)$  is the total stream discharge. Let  $c$  be a conservative isotope tracer with the bulk mass balance:

$$\frac{d(c_s(t)S(t))}{dt} = c_J(t)J(t) - c_{ET}(t)ET(t) - c_t(t)Q_t(t) \quad (2)$$

where  $Q_t$ ,  $c_t$ , and  $c_J$  are the only measured physical quantities. In addition, there are the time points  $t_0, t_1, \dots, t_n$  and time intervals  $[t_0, t_1[, [t_1, t_2[, \dots, [t_{n-1}, t_n[$  that describe the start and end of  $n$  rainfall-runoff events along the time axis. Furthermore, there is a semantic time measure with the intervals  $e$  (event) and  $p$  (pre-event) that can be moved across the rainfall-runoff events, whereas the interval  $p$  is the range of all intervals just before interval  $e$ . The stream discharge  $Q_t$  during event  $e$  is composed of water of the current rainfall-runoff event and of the prior rainfall-runoff events, such that

$$\begin{aligned} Q_t &= Q_e + Q_p \\ c_t Q_t &= c_e Q_e + c_p Q_p \end{aligned} \quad (3)$$

where  $c_e$  and  $c_p$  are bulk tracer concentrations in the event and pre-event components, respectively.

According to Hoeg (2019), the separation of  $n$  time components in stream discharge  $Q_t$  is based on an iterative balance of catchment input and output tracer mass flows along the time axis. Hereby, the volume flows of precipitation  $J$  and evapotranspiration  $ET$  and change in water storage  $S$  are not explicitly involved. Instead, it is postulated that the pre-event water fraction of each rainfall-runoff event is entirely composed of the event water and pre-event water of the last event. Therefore, for a first backward iteration, we have:

$$\begin{aligned} Q_p &= Q_{e-1} + Q_{p-1} \\ c_p Q_p &= c_{e-1} Q_{e-1} + c_{p-1} Q_{p-1} \end{aligned} \quad (4)$$



For  $\tau$  backward iterations, the whole system of the balance equations can be defined as follows:

$$\begin{aligned}
 Q_t &= Q_e + Q_p \\
 c_t Q_t &= c_e Q_e + c_p Q_p \\
 Q_p &= Q_{e-1} + Q_{p-1} \\
 c_p Q_p &= c_{e-1} Q_{e-1} + c_{p-1} Q_{p-1} \\
 Q_{p-1} &= Q_{e-2} + Q_{p-2} \\
 c_{p-1} Q_{p-1} &= c_{e-2} Q_{e-2} + c_{p-2} Q_{p-2} \\
 &\vdots = \vdots \\
 Q_{p-\tau+1} &= Q_{e-\tau} + Q_{p-\tau} \\
 90 \quad c_{p-\tau+1} Q_{p-\tau+1} &= c_{e-\tau} Q_{e-\tau} + c_{p-\tau} Q_{p-\tau}
 \end{aligned} \tag{5}$$

hereby the event components  $Q_e, Q_{e-1} \dots Q_{e-\tau}$  and pre-event components  $Q_p, Q_{p-1} \dots Q_{p-\tau}$  are unknowns, whereas the tracer concentrations  $c_e, c_{e-1}, \dots, c_{e-\tau}$  and  $c_p, c_{p-1}, \dots, c_{p-\tau}$  are known variables.

In the literature, the following criteria are mentioned in relation to the standard two component separation (Sklash and Farvolden (1979), Buttle (1994)), which also apply to the iterative separation model (5):

- 95 1. The isotopic content of the event component is significantly different from that of the pre-event component.
2. The event component maintains a constant isotopic signature in space and time, or any variations can be accounted for.
3. The pre-event component maintains a constant isotopic signature in space and time, or any variations can be accounted for.

The criteria mentioned above represent a subset of the criteria usually belonging to investigations that consider also the flow  
 100 paths of the separated runoff components (Klaus and McDonnell (2013)).

I would like to add another criterion (Criterion 4) that is usually implicitly considered and simply demands that both the event water  $Q_e$  and pre-event water  $Q_p$  cannot be less than zero or larger than the total runoff  $Q_t$ . Given the equations above, this is the case if the tracer concentration in total runoff  $c_t$  is always between that of the event water  $c_e$  and pre-event water  $c_p$ . In the context of separation model (5), it is required for all the backward iterations  $\tau$  that

$$105 \quad c_e < c_t < c_p \quad \vee \quad c_p < c_t < c_e \tag{6}$$

The tracer concentration  $c_t$  is usually directly taken from the stream discharge. By contrast, the determination of  $c_e$  and  $c_p$  is subject to certain assumptions, which are discussed in almost every hydrograph separation study. For instance, in the context of a chronological sequence of rainfall-runoff events, the event water concentration  $c_e$  can be related to the tracer concentration in the precipitation  $c_j$  (see equation (2)), whereas the pre-event water concentration  $c_p$  can be related to the tracer concentration



110 in the stream discharge before the rainfall-runoff event began. The selected methodology to determine  $c_e$  and  $c_p$  will have a significant impact on the results of the hydrograph separation, as I will discuss later.

Based on the knowns  $Q_t, c_t$  and  $c_e, c_{e-1} \dots c_{e-\tau}$  and  $c_p, c_{p-1} \dots c_{p-\tau}$ , we can iteratively derive for  $\tau \in \mathbb{N}$  backward iterations the following solutions:

$$Q_e = Q_t \frac{c_t - c_p}{c_e - c_p} \quad (7)$$

115  $Q_p = Q_t \frac{c_e - c_t}{c_e - c_p} \quad (8)$

$$Q_{e-\tau} = Q_{p-\tau+1} \frac{c_{p-\tau+1} - c_{p-\tau}}{c_{e-\tau} - c_{p-\tau}}, \tau \geq 1 \quad (9)$$

$$Q_{p-\tau} = Q_{p-\tau+1} \frac{c_{e-\tau} - c_{p-\tau+1}}{c_{e-\tau} - c_{p-\tau}}, \tau \geq 1 \quad (10)$$

In addition, from the linear equation system (5), we get the following composition of the stream discharge  $Q_t$ :

$$Q_t = \sum_{i=0}^{\tau} Q_{e-i} + Q_{p-\tau} \quad (11)$$

## 120 2.2 Separated event water response as an estimator for the time varying backward travel time distribution

The iterative separation model (5) can be used to trace event water over a much longer period after the initial event that is being. For the obtained result, I use the term *separated event water response* to emphasize the fact that the traced response relates to the water of exactly one rainfall event. Conceptually, it can be related to the more commonly used term *travel time distribution*. Basically, it can be a time-varying approximation for it.

125 The travel time distribution is the response or breakthrough of an instantaneous, conservative tracer addition over the entire catchment area. It is a probability distribution that can be derived analytically based on the physical assumptions of the system under investigation (Maloszewski and Zuber (1982)). By applying a convolution integral, it can balance the tracer inputs and outputs of equation (2), as follows:

$$c_Q(t) = \int_{-\infty}^t c_J(t_{in}) h(t - t_{in}) dt_{in}, \quad (12)$$

130 where  $h(\varphi)$  is the probability distribution of the travel times  $\varphi$ , and  $t_{in}$  is the injection time of the tracer. On the catchment scale, travel time distributions can serve as fundamental catchment descriptors, revealing information about storage, flow pathways,



and sources of water in a single characteristic (McGuire and McDonnell (2006)). Assuming steady-state conditions, travel time distributions are often interpreted and applied as time invariant, for instance, as a mean over the period under investigation. In addition, travel time distributions are usually inferred using lumped parameter models that simplify the description of a spatially distributed catchment behavior. Of course, there is evidence and knowledge to the contrary (Hrachowitz et al. (2010), McDonnell et al. (2010), Botter (2012), Heidbüchel et al. (2013)).

For non-stationary systems, it makes sense to distinguish between two types of probability density functions: the *forward travel time distribution* and the *backward travel time distribution* (Niemi (1977)). The forward travel time distribution,  $\vec{h}(\varphi, t_{in})$ , is the probability distribution of the travel times  $\varphi$  conditional on the injection time  $t_{in}$  of a volume flow (e.g., precipitation). The backward travel time distribution,  $\overleftarrow{h}(\varphi, t)$ , is the probability distribution of the travel times  $\varphi$  conditional on the exit time  $t$  of a volume flow (e.g., discharge). When the system is in a steady state (constant input/output fluxes), then the forward and backward travel time distributions collapse into a single probability density function (Niemi (1977), Botter et al. (2011), Rinaldo et al. (2011)); otherwise, the following relation (*Niemi's theorem*) applies:

$$\overleftarrow{h}(t - t_{in}, t) Q_t(t) = J(t_{in}) \theta(t_{in}) \vec{h}(t - t_{in}, t_{in}) \quad (13)$$

where  $\theta(t_{in})$  is a partition function that describes the fraction of rainfall  $J(t_{in})$  that ends up as runoff  $Q_t$ . In addition, an age function  $\omega_Q$  can be defined that describes the ratio between the number of water particles with an age in the interval  $(\varphi, \varphi + d\varphi)$  sampled by  $Q_t$  at time  $t$  and the amount of particles with the same age stored in the control volume at that time:

$$\omega_Q(\varphi, t) = \frac{\overleftarrow{h}(\varphi, t)}{\widehat{h}(\varphi, t)} \quad (14)$$

where  $\widehat{h}(\varrho, t)$  is the probability distribution of the residence times  $\varrho$  of the water particles stored within the control volume at time  $t$ .

The age function  $\omega_Q(\varphi, t)$  is an interesting quantity in the sense that the tracer concentrations  $c_e, c_{e-1}, \dots, c_{e-\tau}$  and  $c_p, c_{p-1}, \dots, c_{p-\tau}$  from equation system (5) can be represented as a function of the same. For instance, the pre-event concentration  $c_p$  for the event  $e$  can be calculated as follows:

$$c_p(e) = \int_{-\infty}^{e-1} c_J(t_{in}) \omega_Q(t - t_{in}, t) \widehat{h}(t - t_{in}, t) dt_{in} \quad (15)$$

In addition, the tracer concentrations from the iterative separation model (5) are initially subject to the following assumption:

$$c_p(e) = c_{p-1}(e+1) = \dots = c_{p-\tau}(e+\tau) \quad (16)$$

Therefore, it implicitly follows that the age function  $\omega_Q(\varphi, t)$  should remain stable during the subsequent rainfall-runoff events  $e, e+1, \dots, e+\tau$ , which requires piece wise steady-state conditions, and that is indeed the core message of Criterion 2 and Criterion 3.

The basic procedure to reconstruct the event water response has already been demonstrated in Hoeg (2019), where the single components  $Q_e, Q_{e-1} \dots Q_{e-\tau}$  were arranged in the following way: Assume we are interested in the event water contribution of



event 1 during events 2, 3, and 4. For this case, I can arrange one after the other: the event water  $Q_e$  of event 1, the last event water  $Q_{e-1}$  of event 2, the next-to-last event water  $Q_{e-2}$  of event 3, and the next-to-next-to-last event water  $Q_{e-3}$  of event 4, as illustrated in Figure A1.

165 When referring to the rainfall events  $J_1, J_2, \dots, J_{\tau+1}$  and the related catchment responses  $Q_1, Q_2, \dots, Q_{\tau+1}$ , I can define the *separated event water response* as follows:

$$H_{[t_1, t_2[} := \sum_{k=1}^{\tau+1} Q_{e-k+1}(Q_k) \quad (17)$$

This is the volume flow of water that entered the catchment at interval  $[t_1, t_2[$  with rainfall  $J_1$  and that appears in the stream discharge  $Q$  during interval  $[t_1, t_1+\tau+1[$ , as a result of the rainfall events  $J_1, J_2, \dots, J_{\tau+1}$  and the related catchment responses

170  $Q_1, Q_2, \dots, Q_{\tau+1}$ .

Furthermore, I postulate that the volume-weighted function of the time-varying separated event water response  $H_{[t_i, t_{i+1}[}$  can be considered as an approximation of the time-varying backward travel time distribution,  $\overleftarrow{h}(\varphi, t)$ , on the time interval  $t \in [t_i, t_{i+\tau+1}[$  regarding all water molecules that entered the catchment (the control volume of system (1)) at  $t_{in} \in [t_i, t_{i+1}[$ :

$$\overleftarrow{h}(\varphi, t) \approx \frac{H_{[t_i, t_{i+1}[}}{\int_{t_i}^{t_i+\tau} H_{[t_i, t_{i+1}[}(t) dt} \quad (18)$$

175 respectively

$$\overleftarrow{h}(\varphi, t) \approx \frac{H_e}{\int_e^{e+\tau} H_e(t) dt} \quad (19)$$

regarding the semantic time intervals  $e, e+1, \dots, e+\tau$  on  $\tau$  backward iterations.

Later in the results, which are given in section 3, I systematically compare the *separated event water response* with the *simulated event water response* of the rainfall-runoff model introduced in section 2.4 for different test scenarios. Two of these (sec-  
 180 tion 3.3) are based on time-varying travel time distributions. The *separated event water response* is related to the left hand side of *Niemi's theorem*, that is, equation (13), whereas the *simulated event water response* is related to the right hand side of it.

### 2.3 Condition number and error estimation

For the analysis of field data, the sensitivity of the model plus the input errors of the known variables are usually included in one measure. For instance, Genereux (1998) and Uhlenbrook and Hoeg (2003) demonstrated this based on analytic expressions  
 185 for the case of uncorrelated known variables and assumed uncertainties, that is, a classical Gaussian error propagation. Others, for example, Kuczera and Parent (1998), Joerin et al. (2002), Weiler et al. (2003), Iorgulescu et al. (2007), and Segura et al. (2012), approximated the expected values based on designed field scenarios and the law of large numbers, which is better known as the Monte Carlo method. By contrast, the condition number allows for the focus to be solely placed on the sensitivity of the model.

190 The iterative separation model (5) can also be represented in the form of a linear equation system:

$$Ax = b \quad (20)$$



where  $A$  is a  $n \times n$  coefficient matrix. It is a sparse matrix (band matrix) with entries along and around the main diagonal;  $x$  is a column vector with  $n$  unknown runoff components;  $b$  is a column vector with  $n$  entries and that is equal to zero except for the first two entries. See appendix B for the case of  $\tau = 3$ .

195 For the benchmark tests in section 3, I am interested in a measure that reflects the sensitivity of the relative error of the solution  $x$  to the changes on the right side  $b$ . In addition, the sensitivity of the solution  $x$  to changes in matrix  $A$  is required. This measure is known as the condition of matrix  $A$  (Turing (1948), Stoer (1994), Higham (1995)). Applying the matrix norm  $\|\cdot\|$ , this is defined as follows:

$$\text{cond}(A) := \|A\| \|A^{-1}\| \quad (21)$$

200 For the linear equation system (20), the following estimation for the relative error in  $x$  can be performed (Stoer (1994)):

$$\frac{\|\Delta x\|}{\|x\|} \leq \text{cond}(A) \frac{\|\Delta b\|}{\|b\|}, \quad (22)$$

which means that in the case of a large condition number, small disturbances in  $b$  can lead to larger errors in  $x$ . A similar estimation can be derived for small disturbances in the coefficients of matrix  $A$  in relation to the relative error in  $x$ :

$$\frac{\|\Delta x\|}{\|x\|} \leq \text{cond}(A) \frac{\|\Delta A\|}{\|A\|} + \mathcal{O}(\|\Delta A\|^2) \quad \text{for } \Delta A \rightarrow 0, \quad (23)$$

205 For the interpretation of the results in section 3, the following properties of the condition number are useful (Deuffhard and Hohmann (2019)):

1.  $\text{cond}(A) \geq 1$
2.  $\text{cond}(\gamma A) = \text{cond}(A)$  for all  $\gamma \in \mathbb{R}, \gamma \neq 0$
3.  $A \neq 0$  is singular, if and only if  $\text{cond}(A) = \infty$ , which implies that the corresponding linear equation system (20) has no  
 210 unique solution.

In general, an equation system with a low condition number is said to be *well-conditioned*, while an equation system with a high condition number (much larger than one) is said to be *ill-conditioned*. Note that the relative error of the complete solution  $x$ , which is subject to the vector norm  $\|\cdot\|$ , is estimated, not the relative error of each unknown, which is a single entry of vector  $x$ . In addition, the condition number does not depend on the size of the input error, as is the case with the Gaussian error  
 215 propagation, and for the simulations presented in section 3, no input errors of the known variables are available.

In section 3, I show that a well-conditioned equation system that is an analog of (5) leads to more reliable separation results in many cases. Vice versa, an ill-conditioned system at time step  $t$  might question the applicability of the iterative separation method, regardless of other factors.

Because the relative error of a single component in solution vector  $x$  is not quantified by the condition number, it should be  
 220 not used for the analysis of field data. For this purpose, the Gaussian standard error is the more suitable measure. Nevertheless, the condition number, which is analogous to the Gaussian standard error, can be related to the first order partial derivatives of the linear equation system (20); for instance, it can be shown that

$$\|f'(A)\| \leq \text{cond}(A) \quad (24)$$



## 2.4 Rainfall generator and rainfall-runoff model

225 For the benchmark tests, I use synthetic data generated by a simple rainfall-runoff model that consists of two linear reservoirs, as shown in Figure A2. A linear reservoir is one in which the storage is directly proportional to the outflow (Dooge (1959))

$$S = k Q, \quad (25)$$

where the constant  $k$ , which has the dimension of time, is the average delay time (mean residence time) resulting from an inflow into the reservoir. It has the draining process (Zoch (1934))

$$230 \quad Q(t) = S(t_0) e^{\frac{-(t-t_0)}{k}}, \quad (26)$$

and impulse response function

$$h(t) = \frac{1}{k} e^{\frac{-t}{k}}, \quad (27)$$

from which the outflow rate is obtained by using the convolution integral. I have designed the model such that a fraction  $\eta$  of the outflow  $Q_U$  from the upper reservoir contributes directly to the streamflow  $Q$ , and the complementary fraction  $1 - \eta$

235 recharges the lower reservoir, which contributes to the streamflow at rate  $Q_L$ :

$$Q(J) = Q_L + \eta Q_U \quad (28)$$

A larger  $\eta$  value would result in an immediate model response to rainfall (*flashy* scenario), whereas a lower  $\eta$  value results in a relaxed model response to rainfall (*damped* scenario). The model operates at hourly time steps over a period of four years. The upper reservoir is initialized with a storage water level  $S_U$  of 0.1 mm at time  $t_0$ . It has an initial tracer concentration  $\delta^{18}\text{O}$

240 of -12.5‰. The mean residence time ( $k_U$ ) of the upper reservoir is set to five days, whereas the lower reservoir has a mean residence time ( $k_L$ ) of three months. The tracer mass flows work under the assumption that both reservoirs are well-mixed.

The above model set-up is actually similar to the benchmark model presented in Kirchner (2016) and Kirchner (2019), but it is of a purely stateless and linear nature. In section 3, I make use of these properties by applying the superposition principle to exactly calculate the runoff response for each single rainfall event. In the context of the current investigation, I call it the

245 *simulated event water response*.

In addition, the model linearity allows for applying an instantaneous delayed impulse of parts of the precipitation to simulate a rapid mobilization of pre-event water, that is, for instance,  $Q_{e-1}$  or  $Q_{e-2}$ , during subsequent events. To achieve this, a fraction  $\alpha$  of the precipitation series  $J$  is applied to the rainfall-runoff module at delayed time  $t - t_0$  (Figure A2). In this scenario, the stream discharge is as follows:

$$250 \quad Q(J) = Q((1 - \alpha)J[t]) + Q(\alpha J[t - t_0]) \quad (29)$$

The delayed fraction  $\alpha$  is not a constant value; rather, it is related to the volume of the subsequent rainfall event, such that the delayed rain impulse cannot exceed a specified part ( $\alpha_{\max}$ ) of the subsequent event:

$$\alpha_e = \begin{cases} \alpha_{\max} \frac{\int_{e+1} J[t]dt}{\int_e J[t]dt} & \text{for } \int_e J[t]dt > \int_{e+1} J[t]dt \\ \alpha_{\max} & \text{for } \int_e J[t]dt \leq \int_{e+1} J[t]dt \end{cases} \quad (30)$$



It has been shown in several studies (e.g., Sklash and Farvolden (1979), Buttle (1994), Hinton et al. (1994), Hoeg et al. (2000) Iorgulescu et al. (2007)) that catchments can store water for days, weeks, or months, but then, the catchments will release the water in minutes or hours in response to rainfall inputs. The benchmark model shown in Figure A2 does not describe the complex hydrodynamic processes that lead to this catchment behavior. Nevertheless, in section 3, I show that the iterative separation model (5) is principally able to detect a delayed response of event water and correctly assign it to the corresponding prior rainfall-runoff event.

### 3 Results

In the following, I begin with a controlled sequence of precipitation and tracer inputs to demonstrate the basic behavior of the rainfall-runoff model shown in Figure A2 and the ability of the iterative separation model (5) to correctly assign the model response to the corresponding model inputs, which are expressed by a sufficient match of the simulated and separated event water response. In all test scenarios, three backward iterations ( $\tau = 3$ ) are calculated. In this way, an almost complete reconstruction of the event water response is possible.

In the second section, a random sequence of precipitation and tracer inputs is considered. Hereby, a *flashy* and a *damped* scenario is examined. Finally, a delayed response from parts of the event water can be validated.

For the tracer concentrations in precipitation  $c_j$ , I choose an  $\delta^{18}\text{O}$  interval between  $-20.0\text{‰}$  and  $-5\text{‰}$ . Throughout each rainfall event, the values for  $c_j$  are kept constant and there are no evapotranspiration processes, interception effects, altitude effects, or similar effects. In addition, the linear storages shown in Figure A2 are assumed to be well-mixed, so that

$$c_e(t) = c_j(t) \quad (31)$$

applies to all simulations. The simulated  $\delta^{18}\text{O}$  values for the total runoff are taken as pre-event water compositions  $c_p$  right before the hydrograph rises. All results are accompanied by an error estimator. Here, the condition number of the linear equation system (section 2.3) that belongs to the iterative separation model (5) is calculated at each time step. Based on this, I show that low condition numbers are very often a prerequisite for small deviations between the simulated and separated event water responses. For the first  $\tau = 3$  events, the condition is not defined in the shown test scenarios, because the calculation of the condition number requires a complete coefficient matrix (see appendix B).

For all the test scenarios, the deviation between the total mass input and simulated output, as well as for the tracer mass input and simulated output, is below 0.5%.

#### 3.1 Controlled rainfall and $^{18}\text{O}$ input

##### 3.1.1 Constant $^{18}\text{O}$ signature in precipitation

In the first simulation, I start with a constant isotope signature in precipitation of  $-10\text{‰}$ . Rainfall is assumed at a rate of 4 mm/h for exactly 24 hours every 1.5 months. This interval corresponds to half the mean residence time of the lower reservoir ( $k_L$ ). The rainfall-runoff model operates in the *damped* scenario.



285 Because of the constant  $^{18}\text{O}$  signature in precipitation, the concentration in the total runoff quickly approaches that of the precipitation (see Figure A3). Here, Criterion 1 of the iterative separation model 5 is increasingly violated. As shown in Figure A4, the condition number ( $\text{cond}(A)$ ) and deviation between the simulated and separated event water response ( $\Delta$ ) grow continuously up to high values: more than  $2 \times 10^6$  for the condition number and  $4 \times 10^{-3}$  mm/h for the deviation. The separated event water responses have values below 0.08 mm/h and appear to be smooth during the first events, but there are increasing  
 290 (numerical) instabilities in the last events. This is visible in Figure A5, in which the mean deviation between the simulated event water response and separated event water response is shown in relation to the components  $Q_e$ ,  $Q_{e-1}$ ,  $Q_{e-2}$ , and  $Q_{e-3}$ . There is an initial mean deviation of above 10% related to the initial water storage level  $S_U$  at time  $t_0$ . Obviously, it is not possible to make an exact separation at the beginning of the simulation. Then, until event no. 10, there is a small mean deviation of about 0.01% and a final mean increase up to 10% for the last events. After event 16, the separation increasingly falls apart. Until event 32,  
 295 there are absolute deviations from the simulation on a scale of  $1 \times 10^8$  mm/h.

### 3.1.2 Alternating $^{18}\text{O}$ signature in precipitation

In the second simulation, I continue with an alternating isotope signal in precipitation between -20‰ and -5‰. Again, rainfall occurs at a rate of 4 mm/h for exactly 24 hours every 1.5 months. The rainfall-runoff model operates in the *damped* scenario.

Because of the alternating  $^{18}\text{O}$  signature in precipitation, the concentration in the total runoff cannot approach that of the precipitation (see Figure A6). As mentioned, the simulated  $\delta^{18}\text{O}$  values for the total runoff are taken as pre-event water compositions  $c_p$  right before the hydrograph rises. As a result, Criterion 1 is always met quite well. As shown in Figure A7, the condition number ( $\text{cond}(A)$ ) and deviation between the simulated and separated event water response ( $\Delta$ ) immediately drop  
 300 down to small values: less than 100 for the condition number and  $3 \times 10^{-6}$  mm/h for the deviation. The separated event water responses have values below 0.08 mm/h and look smooth for all the events. This is visible also in Figure A8, in which the mean  
 305 deviation between the simulated event water response and separated event water response is shown in relation to the separated components  $Q_e$ ,  $Q_{e-1}$ ,  $Q_{e-2}$ , and  $Q_{e-3}$ . Again, there is an initial mean deviation of above 10% related to the initial water storage level  $S_U$  at time  $t_0$ . Then, from event 2, there is a small mean deviation of less than 0.05%, and a final mean decrease down to 0.01% for the last events. The separated event water responses approach the simulated ones very well, with absolute deviations from the simulation on a scale below  $3 \times 10^{-6}$  mm/h.

### 3.2 Random rainfall and $^{18}\text{O}$ input

In the third and fourth simulations, I continue with a random isotope signal in precipitation between -20‰ and -5‰. Rain occurs at a maximum rate of 8 mm/h and maximum of three days for every one to two months. The simulation covers a period of four years, the mean annual precipitation is 1254 mm, and the mean annual runoff is 1252 mm.



### 3.2.1 Flashy scenario

315 In the *flashy* scenario, the tracer concentrations for the discharge instantly follow the tracer concentrations in the precipitation (see Figure A9). Criterion 1 is not fulfilled if the tracer concentration in precipitation is similar to the current tracer concentration in the total runoff, and this happens at exactly two time steps:  $t = 8493$  h (event no. 9) and  $t = 32340$  h (event no. 31). As shown in Figure A10, the condition number ( $\text{cond}(A)$ ) and deviation between the simulated and separated event water response ( $\Delta$ ) shows increased values right after  $t = 8493$  h (up to 1583 for the condition number, 0.056 mm/h for the deviation) and  $t = 32340$  h (up to 3441 for the condition number, 0.053 mm/h for the deviation). The separated event water responses have values below 0.08 mm/h and look smooth for all the events. Except for the events 6-9 ( $\Delta = 1121\%$ ), and events 28-31 ( $\Delta = 214\%$ ), the separated event water responses approach the simulated ones quite well, as shown in Figure A11, with a mean deviation between 0.03% and 16%. Very often, there is an increasing deviation for each further backward iteration, that is,  $\Delta_e \leq \Delta_{e-1} \leq \Delta_{e-2} \leq \Delta_{e-3}$ , with values between  $1 \times 10^{-5}\%$  and 16%.

### 325 3.2.2 Damped scenario

In the *damped* scenario, the tracer concentrations in discharge less quickly follow the tracer concentrations in precipitation as in the *flashy* scenario, as shown in Figure A12. Again, Criterion 1 is not fulfilled if the tracer concentration in precipitation is similar to the current tracer concentration in total runoff, and this happens at exactly two time steps:  $t = 8493$  h (event 9) and  $t = 32340$  h (event 31). As shown in Figure A13, the condition number ( $\text{cond}(A)$ ) and the deviation between the simulated and separated event water response ( $\Delta$ ) show increased values right after  $t = 8493$  h (up to 10920 for the condition number, 0.054 mm/h for the deviation) and  $t = 32340$  h (up to 10780 for the condition number, 0.023 mm/h for the deviation). The separated event water responses have values below 0.22 mm/h and look smooth during all the events. Except for the events 6-9 ( $\Delta = 115\%$ ), and events 28-31 ( $\Delta = 25\%$ ), the separated event water responses approach the simulated ones better than in the *flashy* scenario, as shown in Figure A14, with a mean deviation between 0.003% and 1.7%. Very often, there is an increasing deviation for each further backward iteration, that is,  $\Delta_e \leq \Delta_{e-1} \leq \Delta_{e-2} \leq \Delta_{e-3}$ , with values between  $1 \times 10^{-6}\%$  and 1.7%.

By comparing 100 *flashy* scenarios and 100 *damped* scenarios (Table A1), the above observation can be confirmed. In the *damped* scenarios, the separated event water responses approach the simulated ones better than in the *flashy* scenarios, showing a mean of the median values in the deviation of 0.15 % for the *damped* scenario and 1.56 % for the *flashy* scenario.

### 3.3 Random rainfall and $^{18}\text{O}$ input and delayed response of event water

340 In the fifth and sixth simulations, I continue with a random isotope signal in precipitation between -20‰ and -5‰. Here, rainfall occurs at a maximum rate of 8 mm/h and a maximum of three days for exactly every three months. The simulation covers a period of four years, the mean annual precipitation is 615 mm, and the mean annual runoff is 615 mm. The model operates in the *damped* scenario.

In addition, as introduced in section 2.4 and illustrated in Figure A2, a delayed response of the event water is considered, 345 whereas the delay time corresponds exactly to the time interval between the rain events (three months), meaning that the



impulse of each rain event and delayed impulse of the previous event coincide exactly. With this approach, I would like to simulate a situation in which part of the pre-event water is mobilized by the current rain event.

### 3.3.1 Large delayed fraction: $\alpha_{\max} = 0.3$

I start with a large delayed fraction of  $\alpha_{\max} = 0.3$ , which means that a maximum of 30% of the precipitation impulse is shifted by exactly one event interval. Like in the *damped* scenario in section 3.2.2, the tracer concentrations in discharge less quickly follow the tracer concentrations in precipitation as in the *flashy* scenario, as shown in Figure A15. The strongly delayed mobilization of the event water can bring the rainfall-runoff model closer to a violation of Criterion 1 and Criterion 4; this occurs, for example, during event 9, that is, between steps  $t = 17280$  h and  $t = 19440$  h. Here, the tracer concentrations in total runoff  $c_t$  are just between that of the event water  $c_e$  and the pre-event water  $c_p$ . As shown in Figure A16, the condition number (cond(A)) and the deviation between the simulated event water response and separated event water response ( $\Delta$ ) show increased values right after  $t = 17280$  h (up to 950 for the condition number, 0.056 mm/h for the deviation). The separated event water responses have values below 0.20 mm/h and look smooth during all the events. However, only some of them agree well with the simulated ones, as shown in Figure A17, with a mean deviation between 17.4% and 86.0%. The deviations of the single components  $\Delta_e, \Delta_{e-1}, \dots, \Delta_{e-3}$ , vary between between 1.6% and 162.7%.

### 3.3.2 Small delayed fraction: $\alpha_{\max} = 0.05$

I continue with a small delayed fraction of  $\alpha_{\max} = 0.05$ , which means that a maximum of 5% of the precipitation impulse is shifted by exactly one event interval. Like in the *damped* scenario of section 3.2.2, the tracer concentrations in discharge less quickly follow the tracer concentrations in precipitation as in the *flashy* scenario, as shown in Figure A18. The weakly delayed mobilization of the event water leads to less of a violation of Criterion 1 and a clear fulfillment of Criterion 4 during event 9, that is, between steps  $t = 17280$  h and  $t = 19440$  h. Here, the tracer concentrations in total runoff  $c_t$  are clearly between that of the event water  $c_e$  and pre-event water  $c_p$ . As shown in Figure A19, the condition number (cond(A)) and the deviation between the simulated and separated event water response ( $\Delta$ ) show less increased values right after  $t = 17280$  h (up to 679 for the condition number,  $4.9 \times 10^{-3}$  mm/h for the deviation). The separated event water responses have values below 0.20 mm/h and look smooth for all the events. The separated event water responses agree well with the simulated ones, as shown in Figure A20 and Figure A21, with a mean deviation between 2.5% and 7.1%. The deviations of the single components  $\Delta_e, \Delta_{e-1}, \dots, \Delta_{e-3}$ , vary between between 0.2% and 14.7%.

By comparing 200 *damped* scenarios (3200 events) for a range of delayed fractions  $\alpha_{\max}$  between 1% and 30% (Figure A22), the above observations are put into a more positive perspective. For at least half of the events (the median), the separated event water responses approach the simulated ones quite well for the complete range of  $\alpha_{\max}$  values, with a maximum deviation below 14.0%, and a mean deviations below 1.1%. For all calculated deviations, the mean of medians is below 0.3% and the mean of minimum values is below  $1.1 \times 10^{-6}\%$ .



## 4 Discussion

### 4.1 Design and applicability of the rainfall-runoff model

One objective of the current study was to validate the iterative approach of the system (5) based on a simple rainfall-runoff model and synthetic-generated precipitation data. For this purpose, I have chosen a linear approach that enables a fairly accurate, reliable, and fast calculation of the simulated event water response based on the convolution integral.

Furthermore, I have designed the model, such that it can simulate critical situations that, on the one hand, affect the mathematical prerequisites when applying the iterative separation approach and, on the other hand, may play a significant role in field investigations, for instance, a violation of Criterion 1 or Criterion 4. Both situations critically affect the applicability of the iterative hydrograph separation and are often mentioned in tracer-based field studies (Klaus and McDonnell (2013)). Nevertheless, they can be detected or monitored rather easily: the former based on of the condition number and the latter based on equation (6).

A significant difference in the isotopic content of the event and pre-event water component (Criterion 1) is not given, for instance, if rain falling on the catchment with an isotope signature similar to that in the channel network, as it is simulated in section 3.2 for the *flashy* scenario (Figure A9) and the *damped* (Figure A12) scenario, with immediately increased values of the condition number and deviation from the simulated event water response for exactly  $\tau + 1$  events (Figure A10 and Figure A13). In the *damped* scenario, the condition numbers and percentage deviations are lower than in the *flashy* scenario (Figure A11) and Figure A14). The reason for this is obvious: in the *damped* scenario, differences such as  $|c_e - c_p|$  are larger than in the *flashy* scenario.

Because the pre-event water concentration is determined before an event, the isotope composition in the total runoff may not represent a valid mixture of the event water and pre-event water component (Criterion 4) if the proportion of rapidly mobilized pre-event water is relatively large. This is simulated in section 3.3.1 for the *damped* (Figure A15) scenario during event 9. Here, the large fraction (30%) of rapidly mobilized pre-event water influences the isotope signature in the total runoff so strongly that the condition of equation (6) is just met to some extent. A further increase of the delayed fraction  $\alpha_{\max}$  would let the separated event water fraction exceed 100%, whereas the pre-event water fraction would fall below 0%, that is, show negative values. If the isotope composition of the event component does not sufficiently differ from the pre-event component, a violation of Criterion 4 is accompanied by immediately increased values of the condition number and deviation from the simulated event water response for exactly  $\tau + 1$  events (Figure A16 and Figure A17).

Conversely, the iterative separation method performs better for medium and smaller fractions of rapidly mobilized pre-event water ( $\alpha_{\max}$ ), as shown in section 3.3.2. Here, Criterion 4 is consistently fulfilled, and the iterative separation method can reconstruct the complete event water response, as shown in Figure A20 and Figure A21. Nevertheless, for at least half of the events (the median), a good match between the simulated and separated event water responses can be expected for all considered values of  $\alpha_{\max}$  (Figure A22). This is an important capability of the iterative equation system (5), because there are several field studies (Casper et al. (2003), Iorgulescu et al. (2007), James and Roulet (2009)) in which the rapid mobilization of recent water is postulated for events with a higher antecedent moisture.



Although a constant isotopic signature in space and time is maintained for the event and pre-event water component (Criterion 2 and Criterion 3) in all simulations of section 3, it is clear that this does not reflect the complexity of a natural hydrological system. For instance, in the applied rainfall-runoff model in section 2.4 and Figure A2, the tracer mass flows under the assumption that both reservoirs are well mixed, whereas at the catchment scale, there is often a heterogeneous surface and subsurface structure, exposing multiple flow pathways, flow path lengths, and connectivities across different space and time scales (Buttle (1998), Bonell (1998), Uhlenbrook et al. (2002), Li and Sivapalan (2011), Dusek and Vogel (2018)), which would affect the assumption made in Criterion (3). Furthermore, a constant isotopic signature for each simulated event is given as requested in Criterion (2), but under field conditions, intra-storm variabilities of the isotopic composition in precipitation (Kendall and McDonnell (1998)), complex patterns of throughfall depth and water isotopic composition because of interception processes (Saxena (1986), Herbstritt et al. (2019)), along with spatial or temporal variabilities because of altitude effects (Hoeg et al. (2000), Schmieder et al. (2018)) may violate the same.

## 4.2 Applicability of the condition number as error estimator

Initially introduced for the analysis of rounding-off errors (Turing (1948)) and the numerical solvability of linear equation systems (Mallock and Darwin (1933)), the condition of a linear equation system can be regarded as a measure of the sensitivity of the solution of a linear system to the disturbances in the data and as a measure of the sensitivity of the matrix inverse to the disturbances in the matrix. The condition number bounds the level of uncertainty inherent in the solution before a numerical algorithm is applied (Stoer (1994), Higham (1995)). Hence, it helps to evaluate the mathematical constraints that arise directly from the addressed physical model, which is a hydrograph separation model.

In section 3, I have demonstrated that a well-conditioned equation system analogous to (5) leads to more reliable hydrograph separation results in general, whereas an ill-conditioned system at a certain time step might impede the applicability of the iterative hydrograph separation method for the current and subsequent events, here independent of other factors such as uncertainties in the field data. As shown in equations (22) and (23), the condition number stretches an upper bound for the relative error in the solution vector, which might limit the applicability for analyzing the field data. However, because an ill-conditioned system will lead to larger gradients in a Jacobian matrix and to potentially higher errors in a Gaussian error propagation, every tracer-based hydrograph separation should be accompanied by this kind of error analysis. For the standard two component hydrograph separation, this is a common, though sometimes neglected, practice (Bansah and Ali (2017), Kirchner (2019)). Regarding the iterative hydrograph separation method, Jacobian entries for two backward iterations ( $\tau = 2$ ) are published in Hoeg (2019). For arbitrary  $n$ -component systems, the exact analytic expressions are sometimes hard to retrieve or compute; in these cases, a Monte Carlo analysis should be a valid fallback.

## 4.3 Event water response as an estimator for time-varying backward travel time distributions

Jasechko (2019) mentioned that each of the known approaches to determine travel time distributions has advantages and disadvantages and that their usefulness outside of intensively-monitored catchments has yet to be tested. In my opinion, it should be a combination of different perspectives (methods) and additional tracers that can provide an overall picture and



enable balanced decisions. First, the advantages of the iterative separation model (5) are that the approach is easy to use, it  
 445 requires no calibration effort and can deliver useful results regarding a preliminary analysis, and it can provide results for  
 a certain range of problems with low coding and low computational effort. Actually, a simple spreadsheet program such as  
 Microsoft Excel or Open Office Calc would be sufficient to build a first version. However, for the full range of tasks, additional  
 tools and efforts are required, particularly regarding an adequate determination of the known variables, especially the tracer  
 concentrations  $c_e, c_{e-1}, \dots, c_{e-\tau}$  and  $c_p, c_{p-1}, \dots, c_{p-\tau}$ , to address the entire control volume, that is, the catchment. Regardless of  
 450 the selected method, estimating the travel time distribution is associated with a higher computation effort in the non-stationary  
 case. There is currently no hydrological concept or method that can directly solve the problem shown in section 3.3.1. In fact,  
 it is *Niemi's theorem* (equation (13)) that needs to be balanced here.

In section 3, I have demonstrated that the event water response can be interpreted as the breakthrough of an isotope impulse  
 because of a rainfall-runoff event over  $\tau$  subsequent rainfall-runoff events. Based on equation (18), I have postulated that the  
 455 *volume weighted separated event water response* can serve as an estimator for the backward travel time distribution over the  
 current and  $\tau$  subsequent rainfall-runoff events, implying that *recent water* fractions, such as  $Q_{e-1}, Q_{e-2} \dots Q_{e-\tau}$ , can be used to  
 estimate the time-varying structure of the catchment storage.

Regarding the performed *flashy* and *damped* benchmark tests (section 3.2), the above postulate could be very well and easily  
 confirmed, provided that Criterion (1) is sufficiently met. By contrast, regarding the performed *delayed fraction* benchmark tests  
 460 (section 3.3), the above postulate could be confirmed only for the *small* and *medium delayed fraction* scenario, provided that  
 Criterion (1) and Criterion (4) are sufficiently met. One reason is that with an increasing proportion of rapidly mobilized pre-  
 event water, such as  $Q_{e-1}$ , the pre-event water concentration  $c_p$  may decreasingly represent the bulk pre-event concentration of  
 the considered control volume. Please note that in all scenarios shown in section 3, the pre-event concentrations are taken from  
 the stream discharge concentration  $c_t$  right before the hydrograph rises and are assumed to be constant over the entire event.  
 465 Here, intra-storm time-varying values instead of constant concentrations would probably lead to a better match between the  
 simulation and separation. This is demonstrated in Figure A23, where the values  $c_e(e)$  and  $c_{e-1}(e+1)$  are inversely calculated  
 based on the iterative equations system (5) and the *simulated event water response*, that is, the response of the rainfall-runoff  
 model to a specific rainfall event, as follows:

$$c_e = \frac{c_p Q_e + (c_t - c_p) Q_t}{Q_e}$$

$$c_{e-1} = \frac{c_{p-1} Q_{e-1} (c_e - c_p) + c_e Q_t (c_p - c_{p-1}) + c_t Q_t (c_{p-1} - c_p)}{Q_{e-1} (c_e - c_p)} \quad (32)$$

470 It can be seen that for *strong delayed fractions* of the precipitation impulse (with a maximum of 30%), the event water con-  
 centrations of the first subsequent event  $c_{e-1}(e+1)$  are not constant at this point, as it was assumed in the benchmark tests in  
 section 3.3, which is in contrast to the event water concentration of the event related to the precipitation impulse  $c_e(e)$ . Thus,  
 in relation to the bulk mass balance equations (1) and (2), for scenarios with a large fraction of rapidly mobilized pre-event  
 water, it does make sense to express the event water concentration of the prior event  $c_{e-1}(e+1)$  as a function of the tracer con-  
 475 centration in the water storage  $S(t)$  to better represent the bulk pre-event concentration of the considered control volume. For



the *strong delayed fractions* scenario based on the rainfall-runoff model in section 2.4, the *simulated event water response* can be separated by applying the event concentrations  $c_{e-1}(e+1)$  that arise from equation (32). However, to satisfy the complete scenario, an optimization regarding all simulated event water responses would be necessary to find the intra-storm varying tracer concentrations that provide the best results.

480 What about field scenarios in which time dependent variables occur at all time scales and a *simulated event water response* does not exist? Indeed, in catchment hydrology, besides a more intense monitoring of the catchment storage, there are tools that can be used for the appropriate parameterization of intra-storm variations. For instance, because the iterative hydrograph separation model (5) represents a linear system of mass balance equations, it can be connected with the transfer function hydrograph separation approaches introduced by Weiler et al. (2003), Iorgulescu et al. (2007), Segura et al. (2012), or Delsman et al.  
 485 (2013), for example, by identifying process-oriented transfer functions based on Monte Carlo simulations for the unknowns  $Q_e, Q_{e-1} \dots Q_{e-\tau}$ , and  $Q_{p-\tau}$ , to connect the separation results closer to intra-storm related catchment travel times.

In addition, the rate of change of event water  $Q_e$  and recent water  $Q_{e-1}, Q_{e-2} \dots Q_{e-\tau}$  and their contributions to discharge with storage can also be characterized by the age function  $\omega_Q$ , as shown in equation (14). The age function describes the ratio between the number of water particles with an age in a specific time interval sampled in the stream discharge at time  $t$  and the  
 490 amount of particles with the same age stored in the control volume at that time. If we allow event water to be represented by water with age close to the semantic time interval  $e$ , that is,  $t \in e$ , then value  $\omega_Q(e, t)$  scales with the proportion of event water. It is the water delivered to the catchment outlet *instantaneously*, without spending time in storage. On the contrary,  $\omega_Q(e-1, t)$  refers to the water delivered to the catchment outlet *delayingly*, by staying in the catchment storage over the entire event  $e-1$ . Then,  $\omega_Q(e-2, t)$  refers to the water delivered to the catchment outlet *delayingly* by staying in the catchment storage over  
 495 the entire events  $e-2$  and  $e-1$ , and so forth. Regarding a non-stationary problem like the *strong delayed fraction* scenario in section 3.3.1, it would be then necessary to estimate intra-storm variations of the tracer concentrations  $c_e, c_{e-1}, \dots, c_{e-\tau}$  and  $c_p, c_{p-1}, \dots, c_{p-\tau}$  from equation system (5) based on age functions.

Botter (2012) demonstrated how age functions can be used to involve the predominant type of mixing in the catchment and what kind of implications follow for the interpretation of tracer experiments. Based on this consideration, Harman (2015)  
 500 explicitly introduced StorAge Selection (SAS) functions and a dimensionless measure based on the quantity *event water sensitivity* to describe a percent change in event water fraction per change in catchment storage, as a way to better characterize the control of storage on transport. When calculated across a range of hydrologic conditions, the dimensionless measure may be related to fundamental differences in hydrologic flow paths, temporal dynamics of connectivity, and runoff generation mechanisms. Benettin et al. (2017) applied power law based SAS functions and high-resolution isotope data to estimate travel time  
 505 distributions in headwater catchments. With the help of numerical tools and some calibration effort, they were able to reproduce complex measured signals of daily deuterium content in stream waters during wet and dry periods.

Finally, I would like to point out the possibility of connecting the iterative separation model (5) with the *ensemble hydrograph separation* approach introduced by Kirchner (2019). The ensemble hydrograph separation relies on correlations between tracer fluctuations rather than on tracer mass balances. The basic idea, that is, the inclusion of a regression analysis, can be used  
 510 in combination with the separation model (5). In the context of travel time distributions, the ensemble hydrograph separation



approach can be very useful for longer observation periods (months, years, decades), in which the continuous time series of tracer and discharge measurements do not always exist. When looking at the iterative solution in equation (9), this could be achieved by finding a correlation between  $(c_{p-\tau+1} - c_{p-\tau})$  and  $(c_{e-\tau} - c_{p-\tau})$  for a longer observation period. Subgroups of correlations could be retrieved from this, for example, with a seasonal dependency or a relation to antecedent moisture. For the correlation function:

$$F : c_{p-\tau+1} - c_{p-\tau} \mapsto c_{e-\tau} - c_{p-\tau} \quad (33)$$

we finally would get the approximation for  $Q_{e-\tau}$  depending on the observations in the stream only, as follows:

$$Q_{e-\tau} = Q_p \prod_{i=1}^{\tau} \frac{c_{p-\tau+1} - c_{p-\tau}}{F(c_{p-\tau+1} - c_{p-\tau})}, \tau \geq 1 \quad (34)$$

Figure A24 shows the corresponding correlation functions for the scenarios presented in section 3.

## 520 5 Conclusions

A validation of the recently introduced iterative extension of the standard two-component hydrograph separation method was presented. Data were retrieved from a random rainfall generator and a rainfall-runoff model composed of linear reservoirs. The results showed that it is possible to reconstruct the *simulated event water response* for a given model input by using a single stable isotope tracer. It was demonstrated, how mathematical constraints, such as an ill-conditioned linear equation system, may influence a separation of the event water response. It was considered and discussed how the *volume weighted separated event water response* can serve as an estimator for the time-varying backward travel time distribution. The benchmark model also covered the partially delayed response of event water so that a situation was simulated in which pre-event water is rapidly mobilized. Related to this, it was shown that in the case of large fractions of rapidly mobilized pre-event water, a time-varying determination of the pre-event water tracer concentrations to better represent the entire control volume becomes a key aspect.

The results obtained above should provide certainty about the capabilities of the iterative hydrograph separation method. Of course, further validation scenarios with different parameter sets are conceivable. Non-linear rainfall-runoff models can be involved. In addition, further tests with experimental field data would be desirable. The effort will be worth it because the iterative hydrograph separation method is easy to use and requires no calibration effort. It provides immediate results directly from observational data with low coding and low computational effort, and it can be connected with further methods for more detailed analyses and special use cases.

*Code availability.* Once the manuscript is stable during the review process, all the matlab scripts to generate the data and figures shown in section 3 can be accessed at the Open Science Framework <https://osf.io/5uv6e/>.



## Appendix A: Notation

### A1 Latin symbols

	$A$	coefficient matrix of linear equation system
	$b$	column vector of linear equation system
	$c_e$	tracer concentration event water (‰)
	$c_j$	tracer concentration precipitation (‰)
	$c_e$	tracer concentration water storage (‰)
	$c_{ET}$	tracer concentration water vapor (‰)
	$c_p$	tracer concentration pre-event water (‰)
	$ET$	evapotranspiration (mm/h)
	$h$	travel time distribution, impulse response function (-)
	$\overleftarrow{h}$	backward travel time distribution (-)
	$\overrightarrow{h}$	forward travel time distribution (-)
	$\hat{h}$	residence time distribution (-)
	$H$	separated event water response (mm/h)
540	$J$	precipitation (mm/h)
	$k$	mean residence time of a linear reservoir (h)
	$k_L$	mean residence time of the lower reservoir (h)
	$k_U$	mean residence time of the upper reservoir (h)
	$Q$	outflow from linear reservoir (mm/h)
	$Q_e$	event water (mm/h)
	$Q_L$	outflow from lower reservoir (mm/h)
	$Q_p$	pre-event water (mm/h)
	$Q_t$	stream discharge (mm/h)
	$Q_U$	outflow from upper reservoir (mm/h)
	$S$	water storage (mm)
	$t$	time (h)
	$t_{in}$	injection time (h)
	$x$	column vector of linear equation system



## A2 Greek symbols

$\alpha$	delayed fraction of precipitation (-)
$\alpha_{\max}$	maximum delayed fraction of precipitation (-)
$\Delta$	deviation between simulated and separated event water response (mm/h)
$\eta$	fraction of the upper reservoir that contributes directly to the streamflow (-)
$\theta$	partition function (-)
$\tau$	backward iteration (-)
$\varphi$	travel time (h)
$\omega_Q$	age function (-)

## Appendix B: Linear Equation System for three Backward Iterations

The iterative separation model (5) can be represented in the form of a linear equation system for  $\tau = 3$ , as follows:

$$\begin{matrix} 545 \end{matrix}
 \begin{bmatrix} 1 & 1 & 0 & 0 & 0 & 0 & 0 & 0 \\ c_e & c_p & 0 & 0 & 0 & 0 & 0 & 0 \\ 0 & -1 & 1 & 1 & 0 & 0 & 0 & 0 \\ 0 & -c_p & c_{e-1} & c_{p-1} & 0 & 0 & 0 & 0 \\ 0 & 0 & 0 & -1 & 1 & 1 & 0 & 0 \\ 0 & 0 & 0 & -c_{p-1} & c_{e-2} & c_{p-2} & 0 & 0 \\ 0 & 0 & 0 & 0 & 0 & -1 & 1 & 1 \\ 0 & 0 & 0 & 0 & 0 & -c_{p-2} & c_{e-3} & c_{p-3} \end{bmatrix}
 \begin{bmatrix} Q_e \\ Q_p \\ Q_{e-1} \\ Q_{p-1} \\ Q_{e-2} \\ Q_{p-2} \\ Q_{e-3} \\ Q_{p-3} \end{bmatrix}
 =
 \begin{bmatrix} Q_t \\ c_t Q_t \\ 0 \\ 0 \\ 0 \\ 0 \\ 0 \\ 0 \end{bmatrix}
 \quad (B1)$$

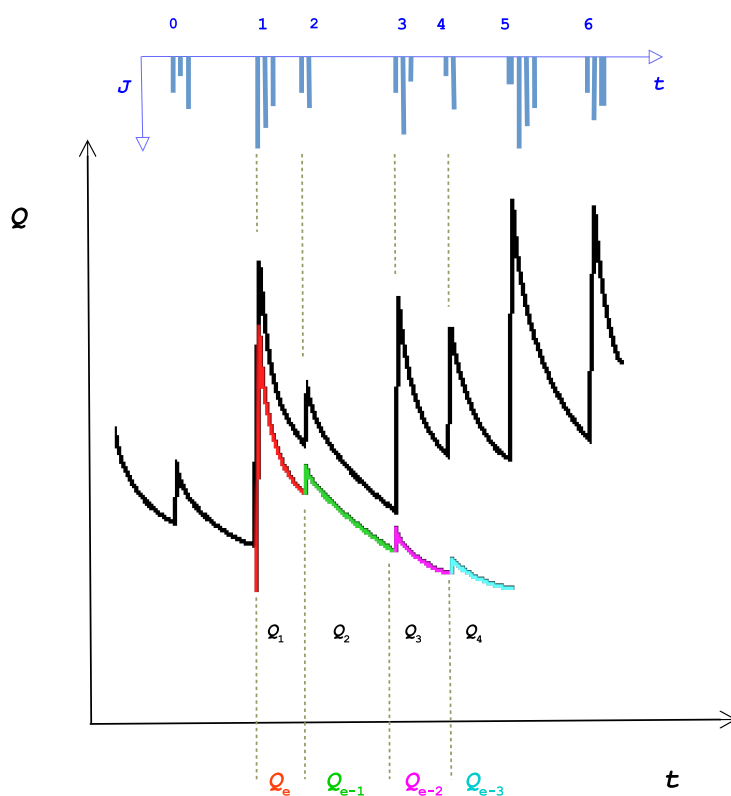


**Figure A1.** Determining the event water response for the rainfall-runoff event  $Q_1(J_1)$  based on the separated runoff components  $Q_e$  (related to  $Q_1(J_1)$ ),  $Q_{e-1}$  (related to  $Q_2(J_2)$ ) ...  $Q_{e-3}$  (related to  $Q_4(J_4)$ ).

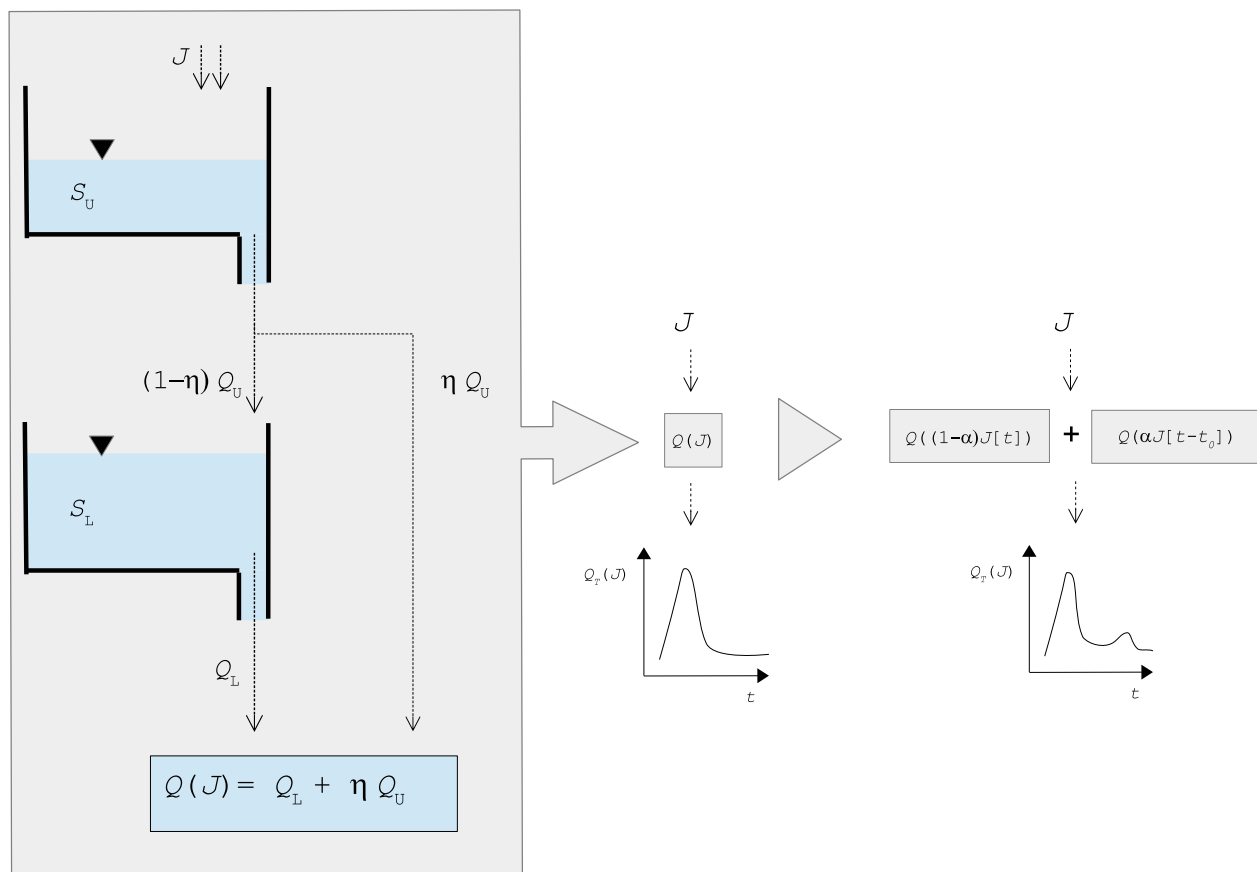


**Figure A2.** Rainfall-runoff model used for the benchmark tests.

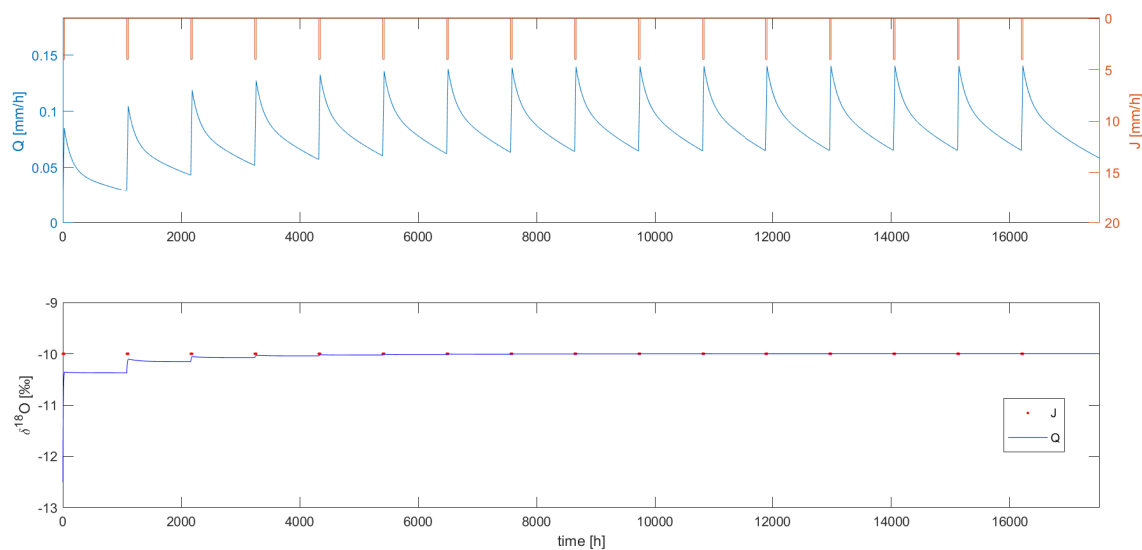


**Figure A3.** Simulation with constant  $^{18}\text{O}$  input - Above: Time series for precipitation  $J$  and total runoff  $Q$  in mm/h. Below: Time series for  $\delta^{18}\text{O}$  values in precipitation  $J$  and total runoff  $Q$  in ‰.

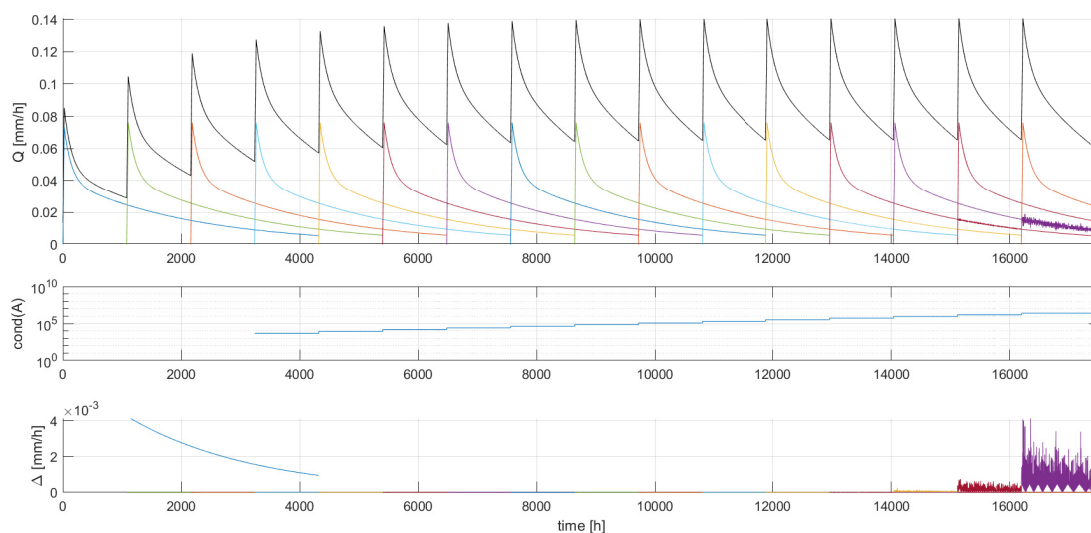


**Figure A4.** Simulation with constant  $^{18}\text{O}$  input - Above: Time series for total runoff  $Q$  in mm/h and the separated event water response for each single event in mm/h. Middle: Condition number ( $\text{cond}(A)$ ) of the iterative separation model (5) for each time step. Below: Deviation between the simulated and separated event water response ( $\Delta$ ) in mm/h.

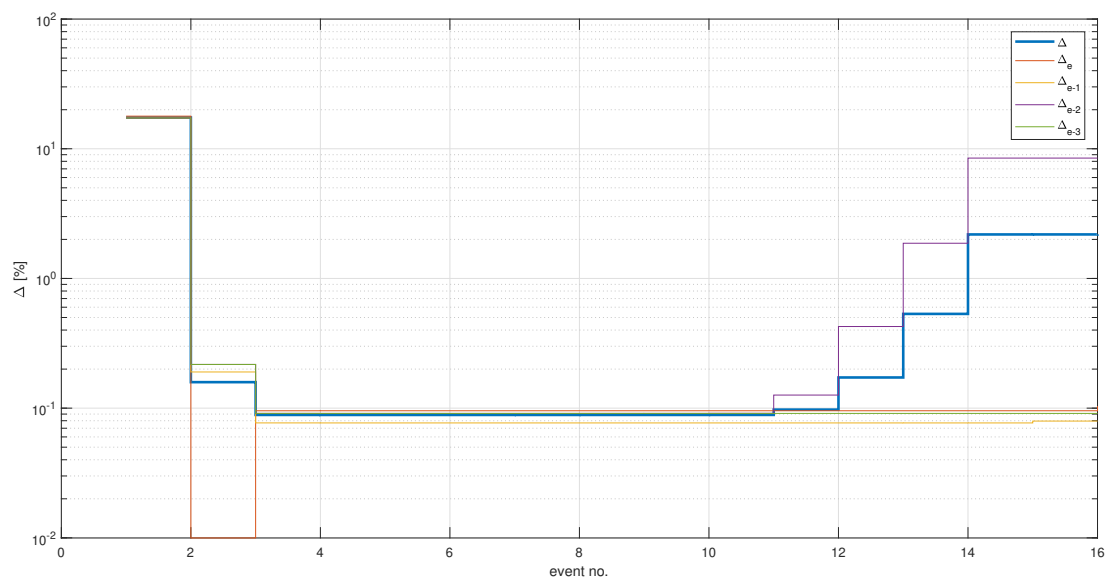


**Figure A5.** Simulation with constant  $^{18}\text{O}$  input - Mean deviation between the simulated event water response and separated event water response for each event in in % -  $\Delta_e$ : Deviation related to  $Q_e$ ,  $\Delta_{e-1}$ : Deviation related to  $Q_{e-1}$ ,  $\Delta_{e-2}$ : Deviation related to  $Q_{e-2}$ ,  $\Delta_{e-3}$ : Deviation related to  $Q_{e-3}$ ,  $\Delta$ : The mean of all deviations.

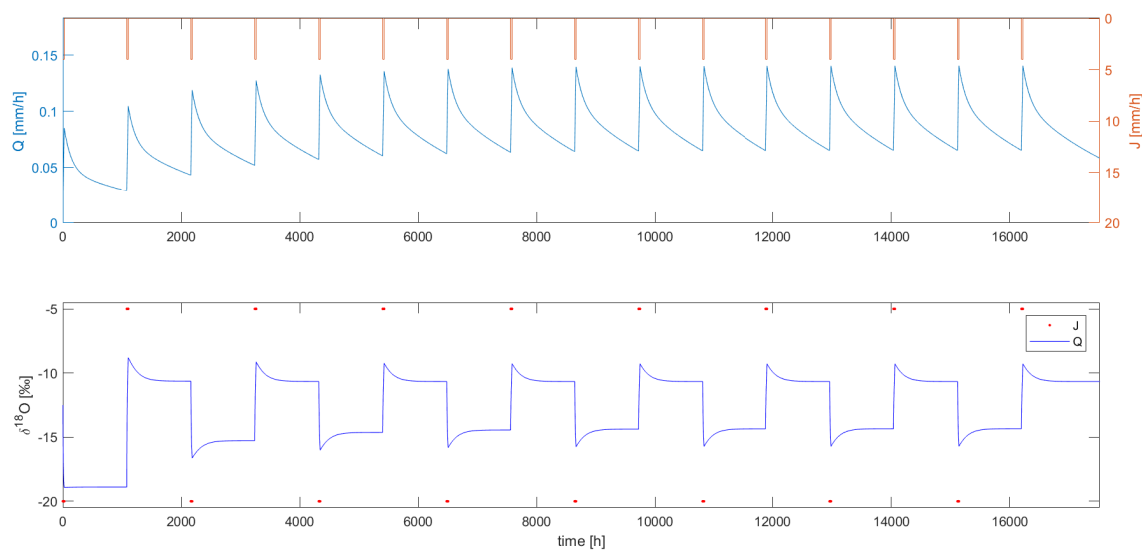


**Figure A6.** Simulation with alternating  $^{18}\text{O}$  input - Above: Time series for precipitation  $J$  and total runoff  $Q$  in mm/h. Below: Time series for  $\delta^{18}\text{O}$  values in precipitation  $J$  and total runoff  $Q$  in ‰.

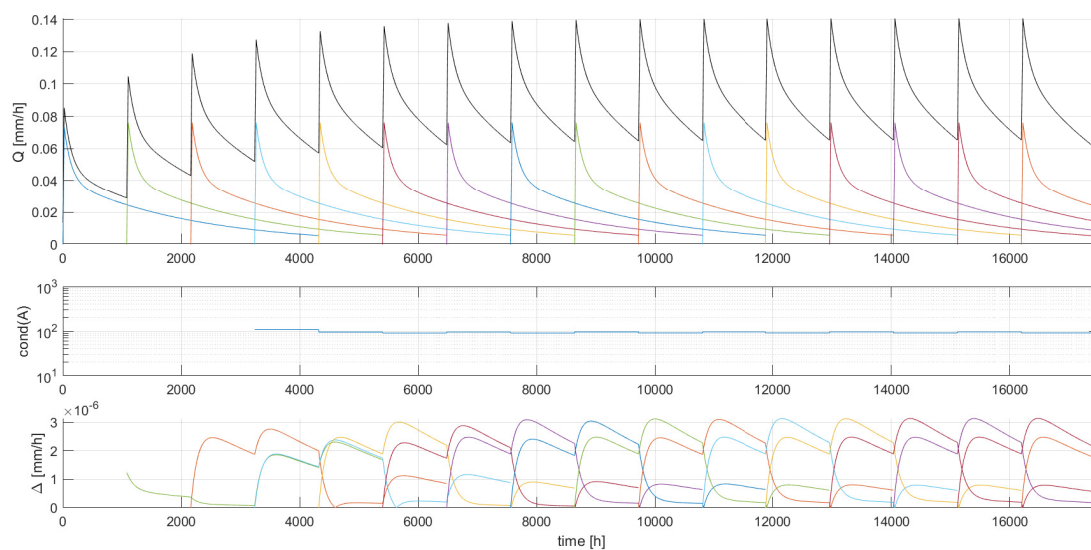


**Figure A7.** Simulation with alternating  $^{18}\text{O}$  input - Above: Time series for total runoff  $Q$  in mm/h and the separated event water response for each single event in mm/h. Middle: Condition number ( $\text{cond}(A)$ ) of the iterative separation model (5) for each time step. Below: Deviation between the simulated and separated event water response ( $\Delta$ ) in mm/h.

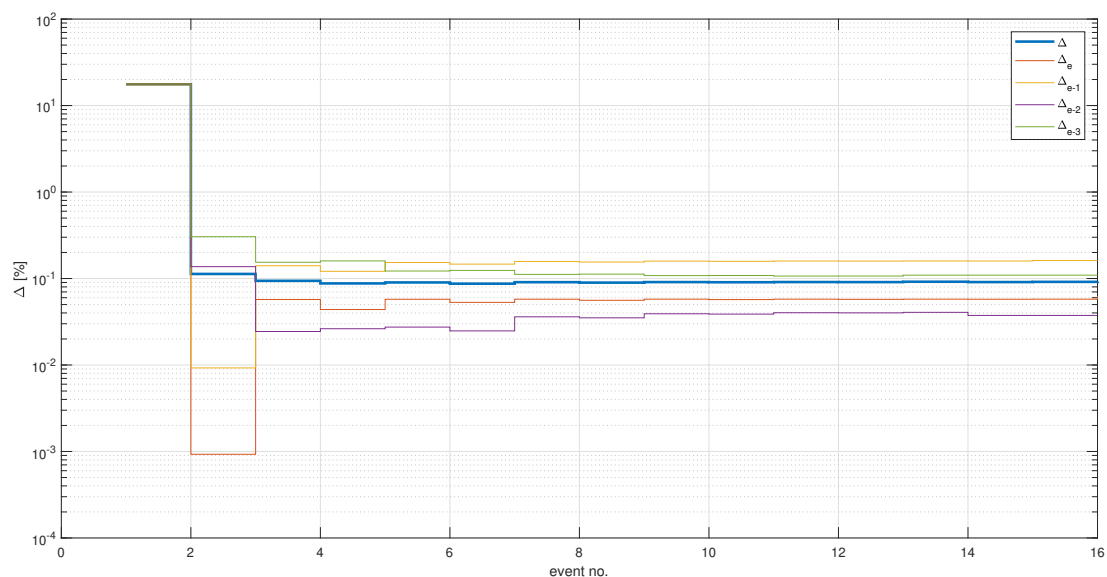


**Figure A8.** Simulation with alternating  $^{18}\text{O}$  input - Mean deviation between the simulated event water response and separated event water response for each event in in % -  $\Delta_e$ : Deviation related to  $Q_e$ ,  $\Delta_{e-1}$ : Deviation related to  $Q_{e-1}$ ,  $\Delta_{e-2}$ : Deviation related to  $Q_{e-2}$ ,  $\Delta_{e-3}$ : Deviation related to  $Q_{e-3}$ ,  $\Delta$ : The mean of all deviations.

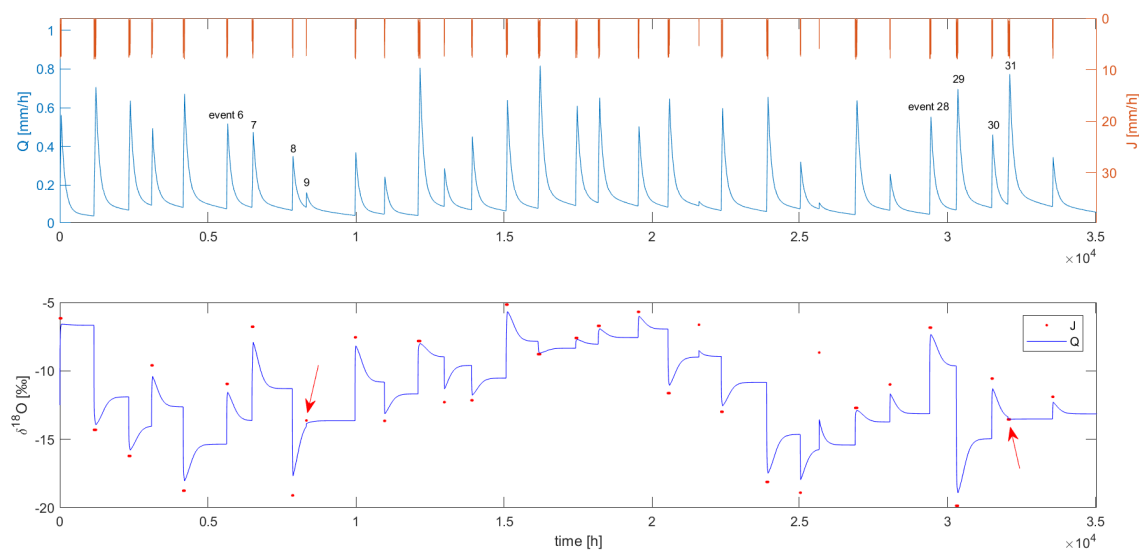


**Figure A9.** Simulation with the *flashy* scenario and random  $^{18}\text{O}$  input - Above: Time series for precipitation  $J$  and total runoff  $Q$  in mm/h. Below: Time series for  $\delta^{18}\text{O}$  values in precipitation  $J$  and total runoff  $Q$  in ‰.

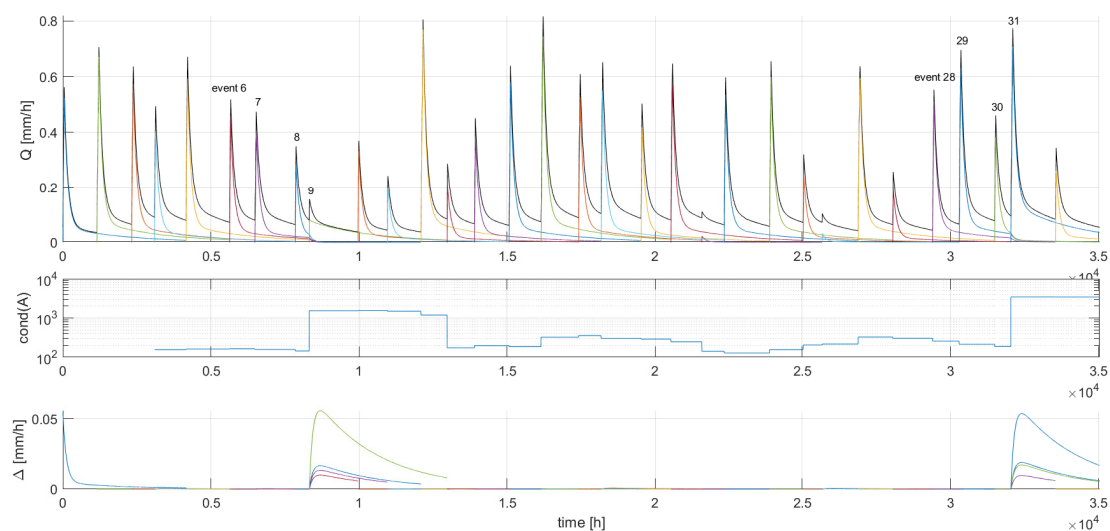


**Figure A10.** Simulation with the *flashy* scenario and random <sup>18</sup>O input - Above: Time series for total runoff  $Q$  in mm/h and the separated event water response for each single event in mm/h. Middle: Condition number ( $\text{cond}(A)$ ) of the iterative separation model (5) for each time step. Below: Deviation between the simulated and separated event water response ( $\Delta$ ) in mm/h.

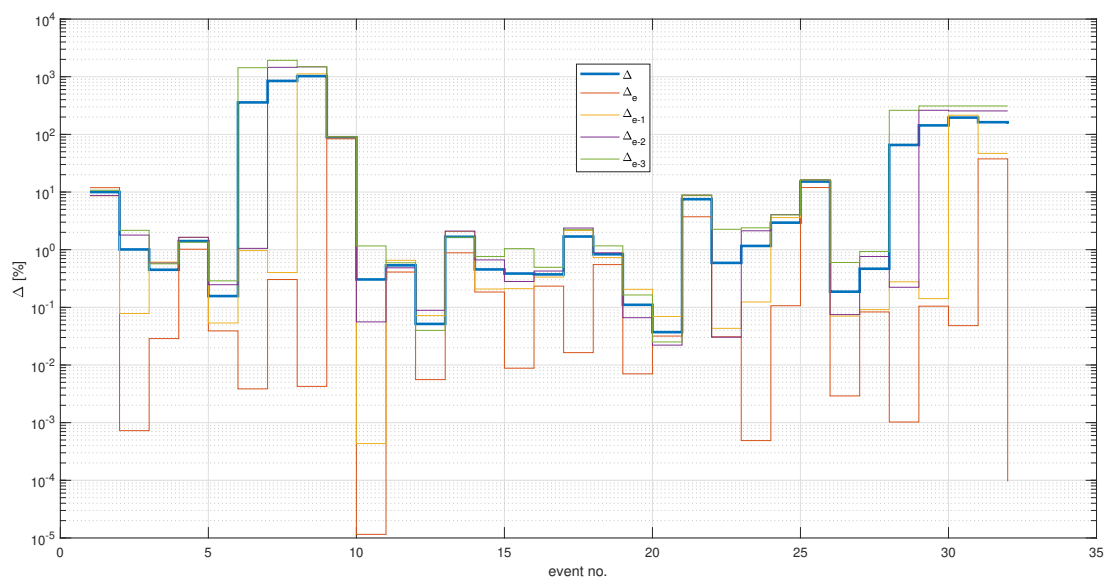


**Figure A11.** Simulation with the *flashy* scenario and random  $^{18}\text{O}$  input - Mean deviation between the simulated event water response and separated event water response for each event in % -  $\Delta_e$ : Deviation related to  $Q_e$ ,  $\Delta_{e-1}$ : Deviation related to  $Q_{e-1}$ ,  $\Delta_{e-2}$ : Deviation related to  $Q_{e-2}$ ,  $\Delta_{e-3}$ : Deviation related to  $Q_{e-3}$ ,  $\Delta$ : The mean of all deviations.

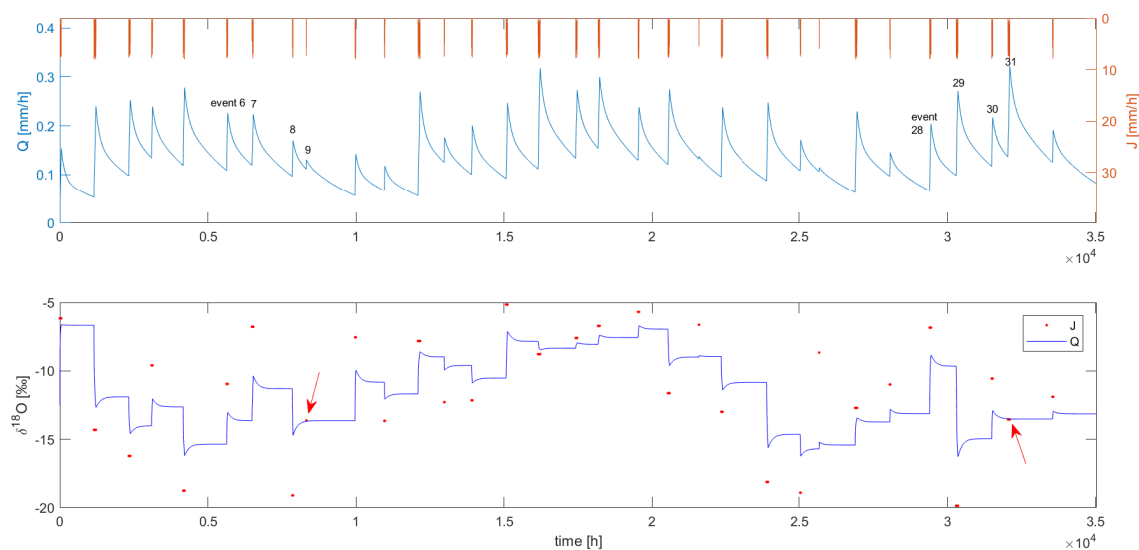


**Figure A12.** Simulation with the *damped* scenario and random  $^{18}\text{O}$  input - Above: Time series for precipitation  $J$  and total runoff  $Q$  in mm/h. Below: Time series for  $\delta^{18}\text{O}$  values in precipitation  $J$  and total runoff  $Q$  in ‰.

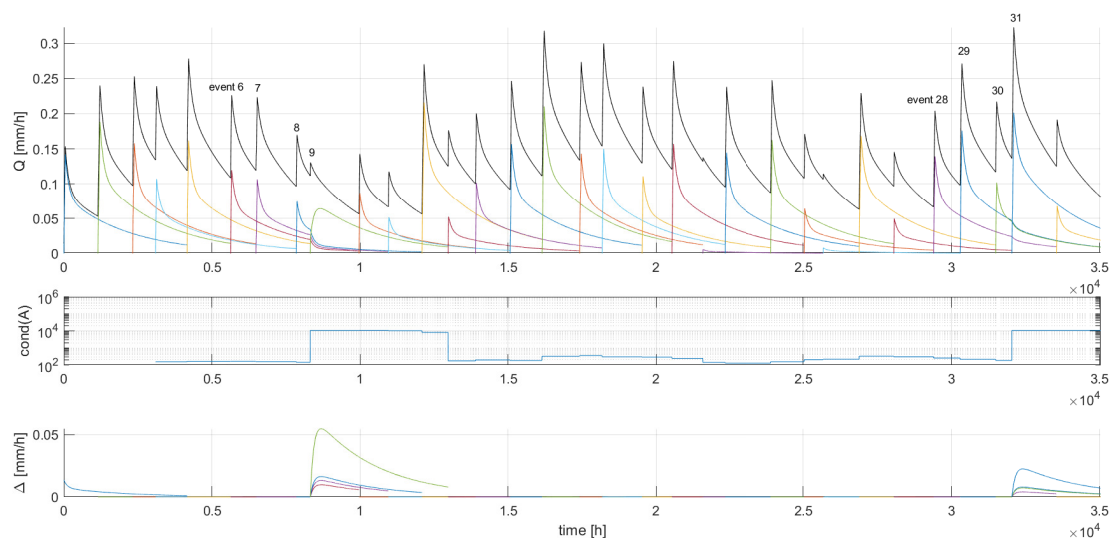


**Figure A13.** Simulation with the *damped* scenario and random  $^{18}\text{O}$  input - Above: Time series for total runoff  $Q$  in mm/h and the separated event water response for each single event in mm/h. Middle: Condition number ( $\text{cond}(A)$ ) of the iterative separation model (5) for each time step. Below: Deviation between the simulated and separated event water response ( $\Delta$ ) in mm/h.

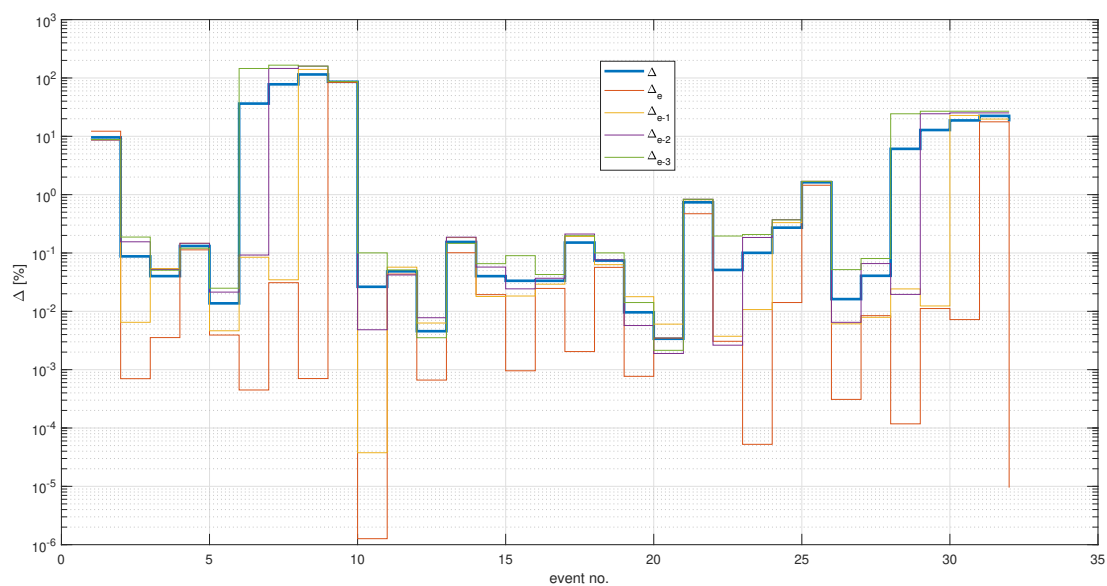


**Figure A14.** Simulation with the *damped* scenario and random  $^{18}\text{O}$  input - Mean deviation between the simulated event water response and separated event water response for each event in % -  $\Delta_e$ : Deviation related to  $Q_e$ ,  $\Delta_{e-1}$ : Deviation related to  $Q_{e-1}$ ,  $\Delta_{e-2}$ : Deviation related to  $Q_{e-2}$ ,  $\Delta_{e-3}$ : Deviation related to  $Q_{e-3}$ ,  $\Delta$ : The mean of all deviations.

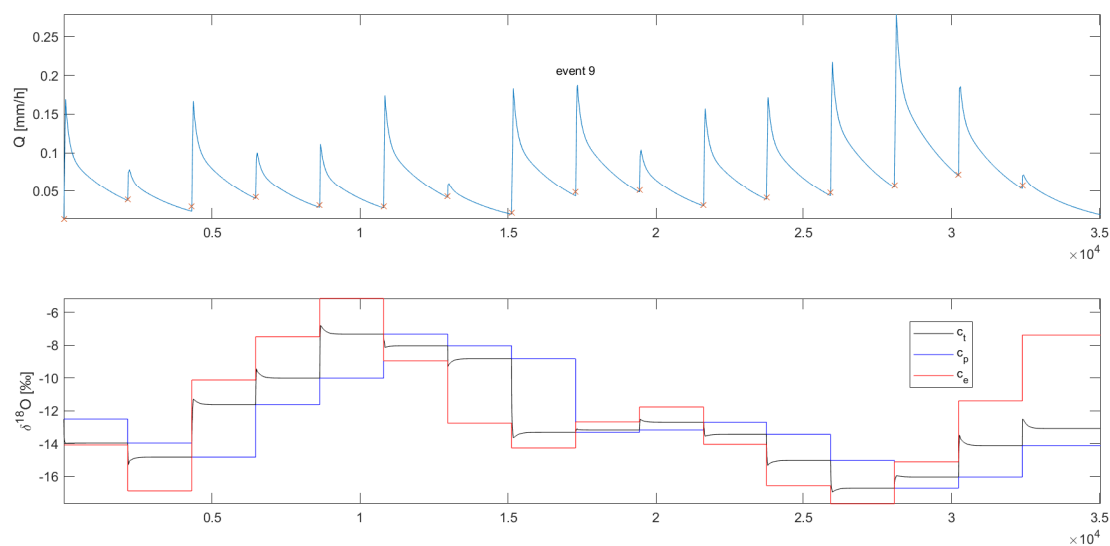


**Figure A15.** Simulation with the *damped* scenario and random  $^{18}\text{O}$  strongly delayed input - Above: Time series for precipitation  $J$  and total runoff  $Q$  in  $\text{mm/h}$ . Below: Time series for  $\delta^{18}\text{O}$  values in precipitation  $J$  and total runoff  $Q$  in  $\text{‰}$ .

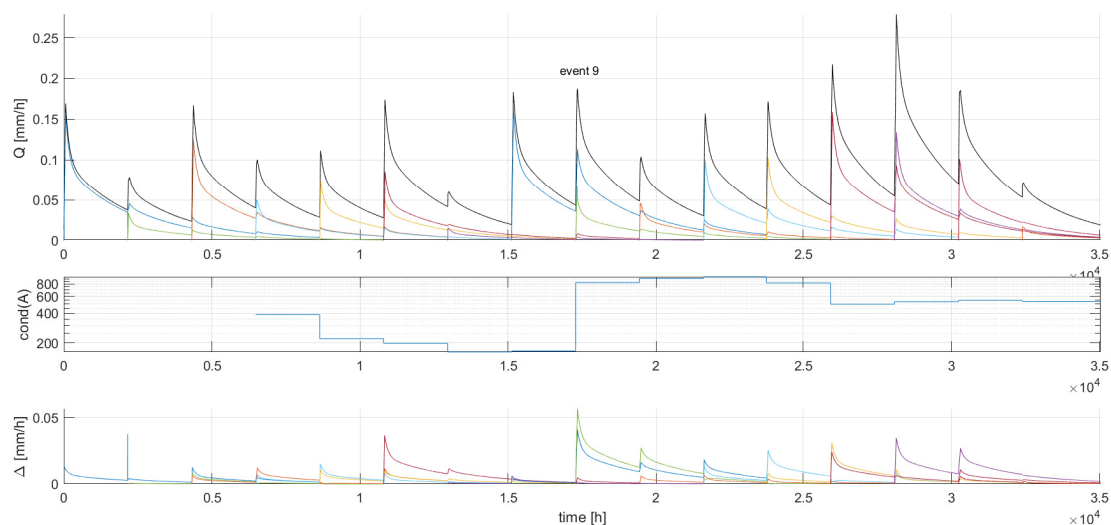


**Figure A16.** Simulation with the *damped* scenario and random  $^{18}\text{O}$  strongly delayed input - Above: Time series for total runoff  $Q$  in mm/h and the separated event water response for each single event in mm/h. Middle: Condition number ( $\text{cond}(A)$ ) of the iterative separation model (5) for each time step. Below: Deviation between the simulated and separated event water response ( $\Delta$ ) in mm/h.

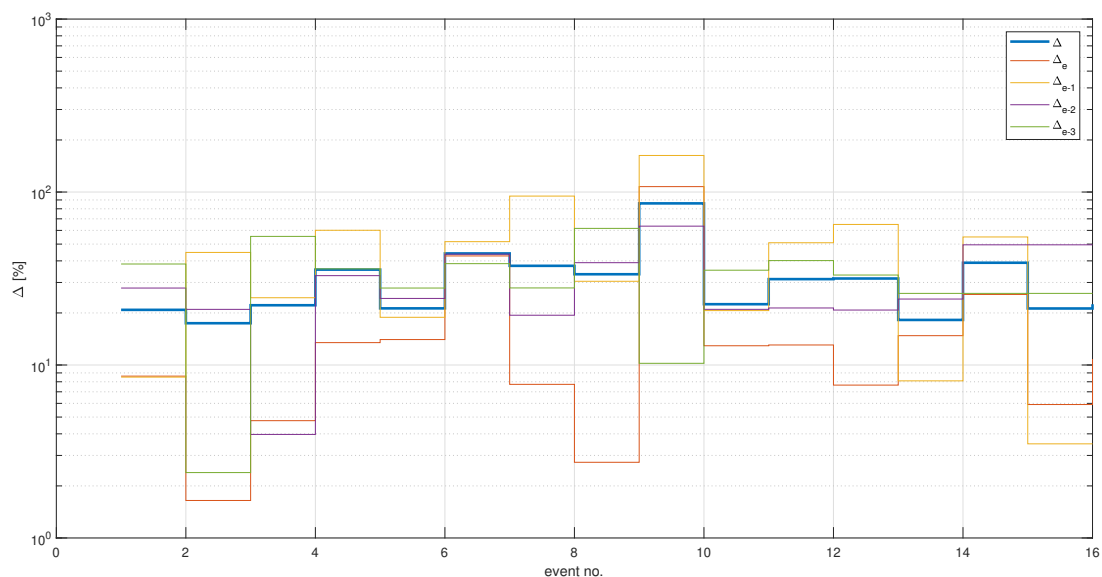


**Figure A17.** Simulation with the *damped* scenario and random  $^{18}\text{O}$  strongly delayed input - Mean deviation between the simulated event water response and separated event water response for each event in % -  $\Delta_e$ : Deviation related to  $Q_e$ ,  $\Delta_{e-1}$ : Deviation related to  $Q_{e-1}$ ,  $\Delta_{e-2}$ : Deviation related to  $Q_{e-2}$ ,  $\Delta_{e-3}$ : Deviation related to  $Q_{e-3}$ ,  $\Delta$ : The mean of all deviations.

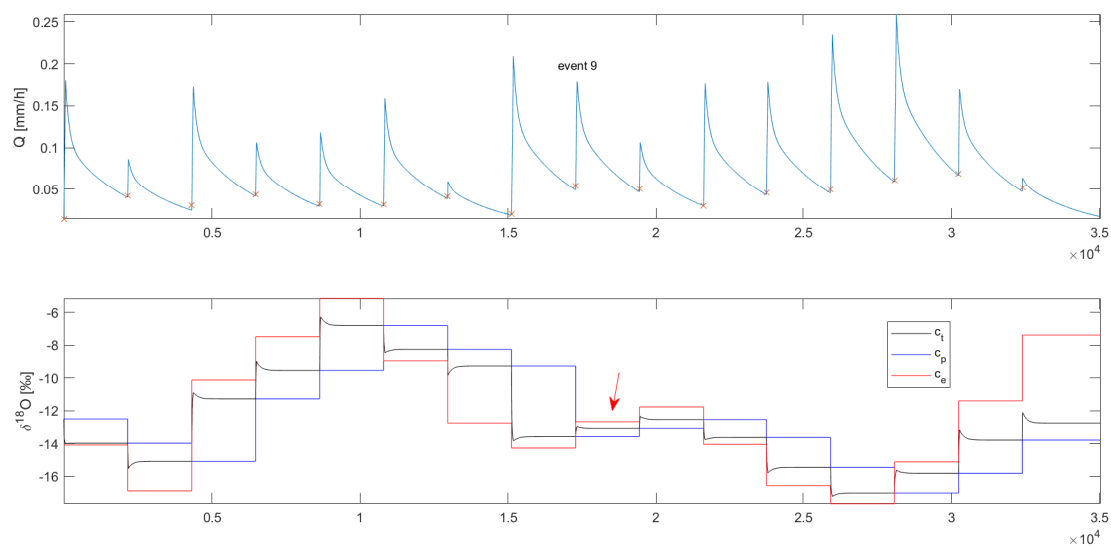


**Figure A18.** Simulation with the *damped* scenario and random  $^{18}\text{O}$  weakly delayed input - Above: Time series for precipitation  $J$  and total runoff  $Q$  in  $\text{mm/h}$ . Below: Time series for  $\delta^{18}\text{O}$  values in precipitation  $J$  and total runoff  $Q$  in  $\text{‰}$ .

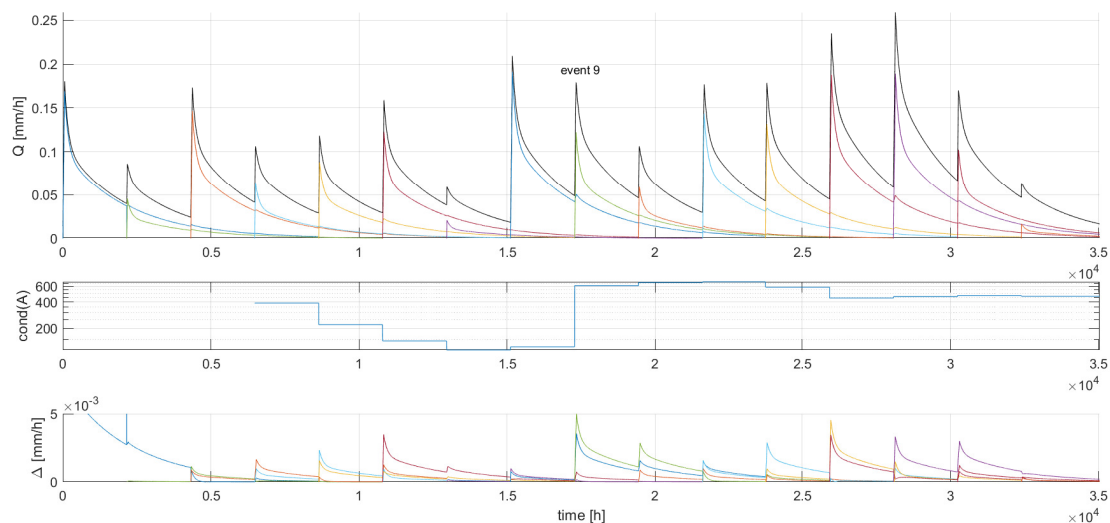


**Figure A19.** Simulation with the *damped* scenario and random <sup>18</sup>O weakly delayed input - Above: Time series for total runoff  $Q$  in mm/h and the separated event water response for each single event in mm/h. Middle: Condition number ( $\text{cond}(A)$ ) of the iterative separation model (5) for each time step. Below: Deviation between the simulated and separated event water response ( $\Delta$ ) in mm/h.

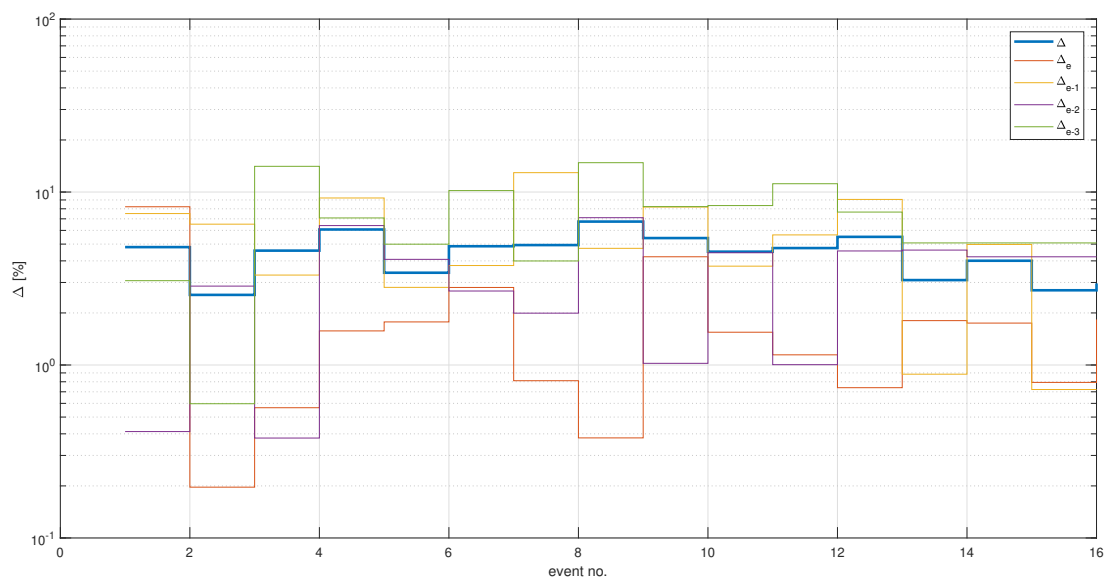


**Figure A20.** Simulation with the *damped* scenario and random  $^{18}\text{O}$  weakly delayed input - Mean deviation between the simulated event water response and separated event water response for each event in % -  $\Delta_e$ : Deviation related to  $Q_e$ ,  $\Delta_{e-1}$ : Deviation related to  $Q_{e-1}$ ,  $\Delta_{e-2}$ : Deviation related to  $Q_{e-2}$ ,  $\Delta_{e-3}$ : Deviation related to  $Q_{e-3}$ ,  $\Delta$ : The mean of all deviations.

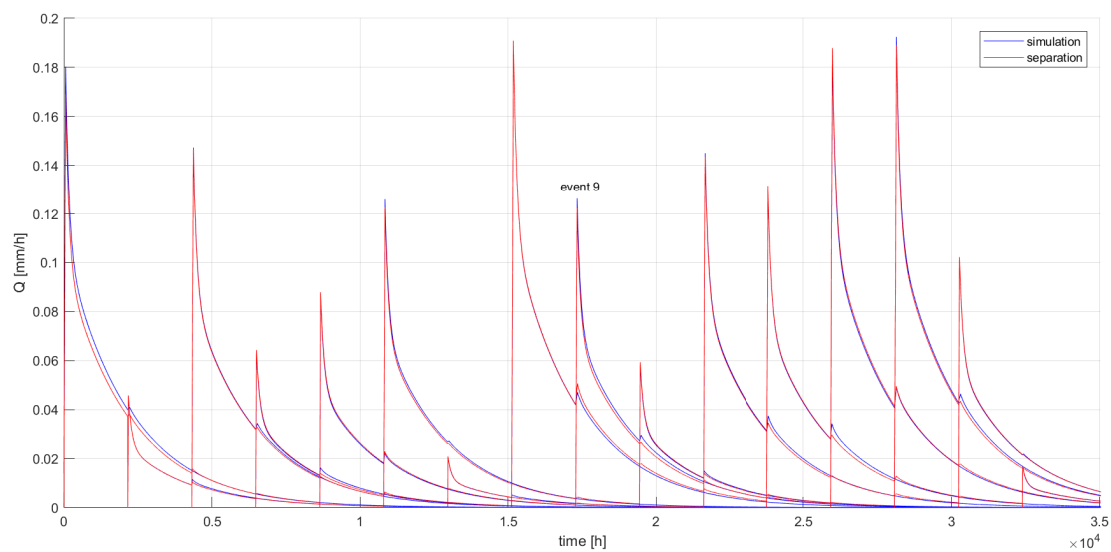


**Figure A21.** Simulation with the *damped* scenario and random  $^{18}\text{O}$  weakly delayed input - Simulated and separated event water responses for all events.

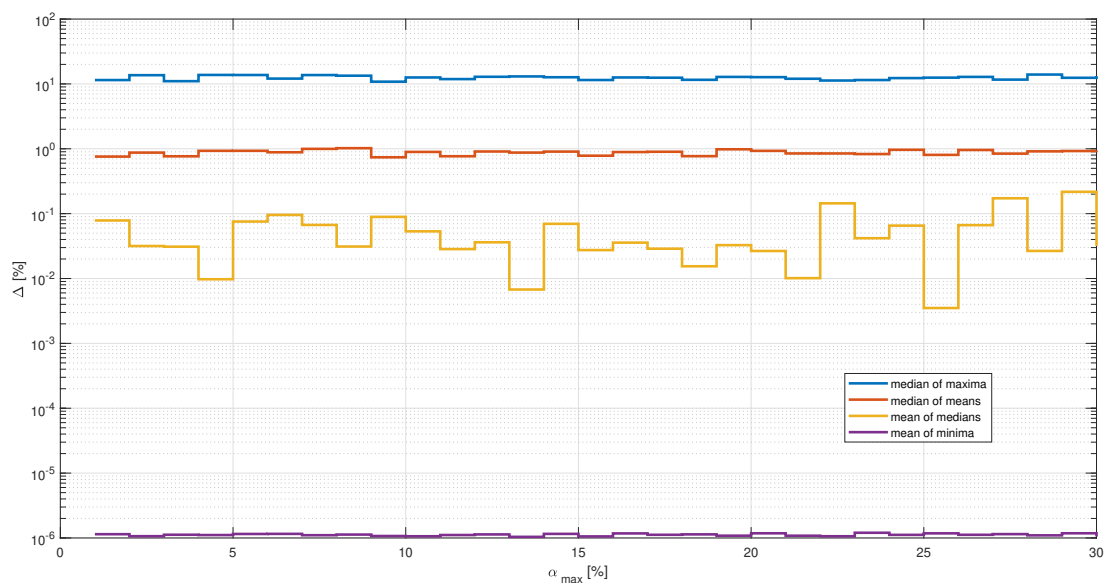


**Figure A22.** *Damped* scenario and random  $^{18}\text{O}$  delayed input - Deviation ( $\Delta$ ) between the simulated and separated event water response for a range of delayed fractions ( $\alpha_{\max}$ ) between 1% and 30% based on 200 simulations (3200 events) for each step - Median of maximum values, median of mean values, mean of median values, and mean of minimum values in %.

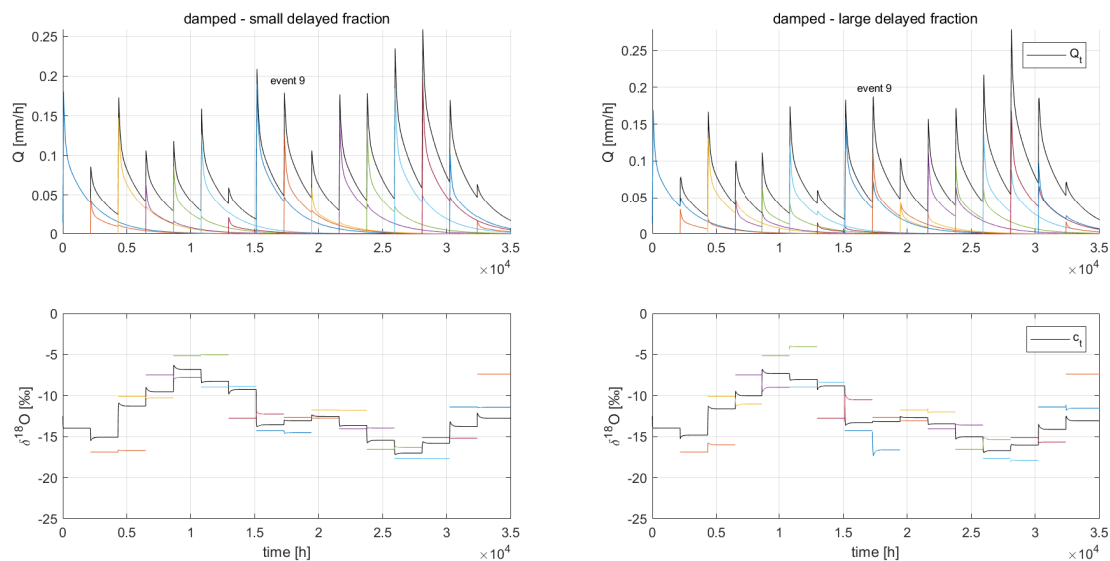


**Figure A23.** Left: *Damped* scenario and random  $^{18}\text{O}$  input plus a small delayed fraction ( $\alpha_{\max} = 0.05$ ) of the precipitation impulse - Right: *Damped* scenario and random  $^{18}\text{O}$  input plus a large delayed fraction ( $\alpha_{\max} = 0.30$ ) of the precipitation impulse - Above: Time series for total runoff  $Q$  in mm/h and the *simulated event water response* for each single event in mm/h. Below: Inversely calculated event water concentrations (in ‰) for each single event  $c_e(e)$  and the first subsequent event  $c_{e-1}(e+1)$  based on the *simulated event water response*.

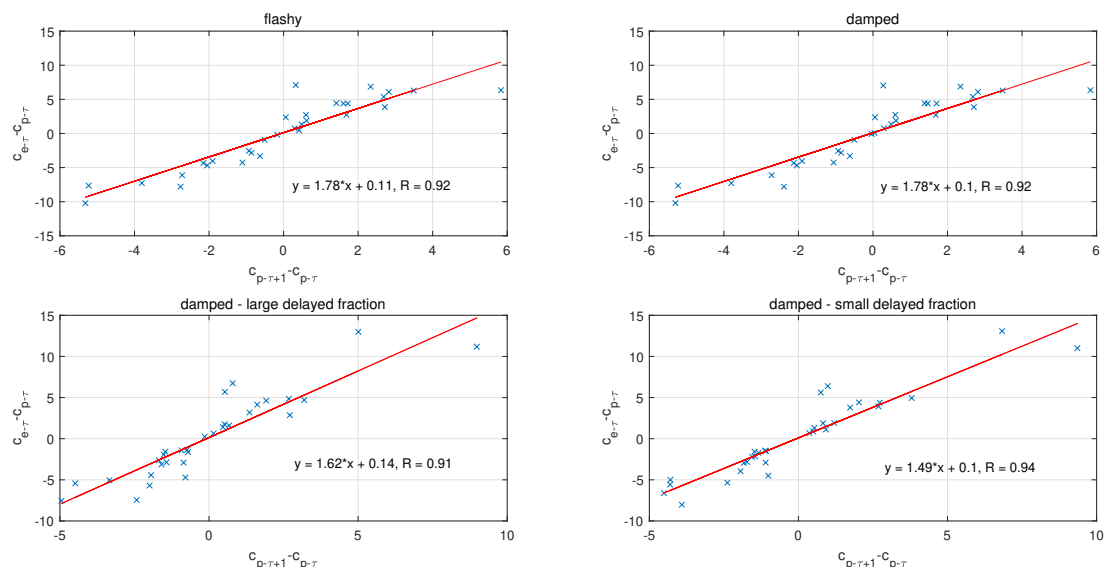


**Figure A24.** Correlation functions according to equation (33) for the *ensemble hydrograph separation* approach regarding the scenarios shown in the results section based on 32 rainfall-runoff events: flashy scenario (section 3.2.1), damped scenario (section 3.2.2), damped scenario with large delayed fraction of event water (section 3.3.1), and damped scenario with small delayed fraction of event water (section 3.3.2).



**Table A1.** Deviation  $\Delta$  between the simulated and separated event water response for the *flashy* scenario and the *damped* scenario based on 100 random rainfall and  $^{18}\text{O}$  input simulations (3200 events): mean of median values, mean of minimum values, median of mean values, and median of maximum values. Deviation  $\Delta$  between the simulated and separated event water response for the *flashy* and *damped* scenario plus *delayed response of event water* based on 200 x 30 random rainfall and  $^{18}\text{O}$  input simulations (3200 x 30 events) for  $\alpha_{\max}$  between 1% and 30%: mean of median values, mean of minimum values, median of mean values, and median of maximum values.

scenario	mean of medians [%]	mean of minima [%]	median of means [%]	median of maxima [%]
<i>flashy</i>	1.56	0.07	4.65	42.37
<i>damped</i>	0.15	0.01	1.08	14.17
<i>flashy + delayed response</i>	< 0.09	< 1.3e-5	< 0.90	< 13.02
<i>damped + delayed response</i>	< 0.22	< 1.2e-6	< 1.03	< 13.95

*Author contributions.* The author prepared the concept, computations, text, tables, and figures for this manuscript

*Competing interests.* The author declares that there are no competing interests

*Acknowledgements.* tbd



## References

- Bansah, S. and Ali, G.: Evaluating the Effects of Tracer Choice and End-Member Definitions on Hydrograph Separation Results Across Nested, Seasonally Cold Watersheds, *Water Resources Research*, 53, 8851–8871, <https://doi.org/10.1002/2016WR020252>, 2017.
- Barthold, F. K., Tyralla, C., Schneider, K., Vaché, K. B., Frede, H.-G., and Breuer, L.: How many tracers do we need for end member mixing analysis (EMMA)? A sensitivity analysis, *Water Resources Research*, 47, <https://doi.org/10.1029/2011WR010604>, 2011.
- Benettin, P., Soulsby, C., Birkel, C., Tetzlaff, D., Botter, G., and Rinaldo, A.: Using SAS functions and high-resolution isotope data to unravel travel time distributions in headwater catchments, *Water Resources Research*, 53, 1864–1878, <https://doi.org/https://doi.org/10.1002/2016WR020117>, 2017.
- Bonell, M.: SELECTED CHALLENGES IN RUNOFF GENERATION RESEARCH IN FORESTS FROM THE HILLSLOPE TO HEADWATER DRAINAGE BASIN SCALE1, *JAWRA Journal of the American Water Resources Association*, 34, 765–785, <https://doi.org/10.1111/j.1752-1688.1998.tb01514.x>, 1998.
- Botter, G.: Catchment mixing processes and travel time distributions, *Water Resources Research*, 48, <https://doi.org/10.1029/2011WR011160>, 2012.
- Botter, G., Bertuzzo, E., and Rinaldo, A.: Catchment residence and travel time distributions: The master equation, *Geophysical Research Letters*, 38, <https://doi.org/10.1029/2011GL047666>, 2011.
- Brown, V. A., McDonnell, J. J., Burns, D. A., and Kendall, C.: The role of event water, a rapid shallow flow component, and catchment size in summer stormflow, *Journal of Hydrology*, 217, 171 – 190, [https://doi.org/https://doi.org/10.1016/S0022-1694\(98\)00247-9](https://doi.org/https://doi.org/10.1016/S0022-1694(98)00247-9), 1999.
- Buttle, J.: Isotope hydrograph separations and rapid delivery of pre-event water from drainage basins, *Progress in Physical Geography: Earth and Environment*, 18, 16–41, <https://doi.org/10.1177/030913339401800102>, 1994.
- Buttle, J.: Chapter 1 - Fundamentals of Small Catchment Hydrology, in: *Isotope Tracers in Catchment Hydrology*, edited by KENDALL, C. and McDONNELL, J. J., pp. 1 – 49, Elsevier, Amsterdam, <https://doi.org/https://doi.org/10.1016/B978-0-444-81546-0.50008-2>, 1998.
- Casper, M. C., Volkmann, H. N., Waldenmeyer, G., and Plate, E. J.: The separation of flow pathways in a sandstone catchment of the Northern Black Forest using DOC and a nested Approach, *Physics and Chemistry of the Earth, Parts A/B/C*, 28, 269 – 275, [https://doi.org/https://doi.org/10.1016/S1474-7065\(03\)00037-8](https://doi.org/https://doi.org/10.1016/S1474-7065(03)00037-8), 2003.
- Christophersen, N. and Hooper, R. P.: Multivariate analysis of stream water chemical data: The use of principal components analysis for the end-member mixing problem, *Water Resources Research*, 28, 99–107, <https://doi.org/10.1029/91WR02518>, 1992.
- Christophersen, N., Neal, C., Hooper, R. P., Vogt, R. D., and Andersen, S.: Modelling streamwater chemistry as a mixture of soilwater end-members — A step towards second-generation acidification models, *Journal of Hydrology*, 116, 307 – 320, 1990.
- Delsman, J. R., Essink, G. H. P. O., Beven, K. J., and Stuyfzand, P. J.: Uncertainty estimation of end-member mixing using generalized likelihood uncertainty estimation (GLUE), applied in a lowland catchment, *Water Resources Research*, 49, 4792–4806, 2013.
- Deuffhard, P. and Hohmann, A.: *Numerische Mathematik 1*, De Gruyter, Walter de Gruyter GmbH, Berlin/Boston, 2019.
- Dincer, T., Payne, B. R., Florkowski, T., Martinec, J., and Tongiorgi, E.: Snowmelt runoff from measurements of tritium and oxygen-18, *Water Resources Research*, 6, 110–124, <https://doi.org/10.1029/WR006i001p00110>, 1970.
- Dooge, J. C. I.: A general theory of the unit hydrograph, *Journal of Geophysical Research* (1896-1977), 64, 241–256, <https://doi.org/10.1029/JZ064i002p00241>, 1959.
- Dusek, J. and Vogel, T.: Hillslope hydrograph separation: The effects of variable isotopic signatures and hydrodynamic mixing in macroporous soil, *Journal of Hydrology*, 563, 446 – 459, 2018.



- Freeze, R. A.: Streamflow generation, *Reviews of Geophysics*, 12, 627–647, <https://doi.org/10.1029/RG012i004p00627>, 1974.
- Fritz, P., Cherry, J., Sklash, M., and Weyer, K.: Storm runoff analysis using environmental isotopes and major ions, in: Advisory group meeting on interpretation of environmental isotope and hydrochemical data in groundwater hydrology, vol. 8, pp. 111–130, International Atomic Energy Agency (IAEA), 1976.
- 590 Genereux, D.: Quantifying uncertainty in tracer-based hydrograph separations, *Water Resources Research*, 34, 915–919, <https://doi.org/10.1029/98WR00010>, 1998.
- Harman, C. J.: Time-variable transit time distributions and transport: Theory and application to storage-dependent transport of chloride in a watershed, *Water Resources Research*, 51, 1–30, <https://doi.org/10.1002/2014WR015707>, 2015.
- Heidbüchel, I., Troch, P. A., and Lyon, S. W.: Separating physical and meteorological controls of variable transit times in zero-order catch-  
 595 ments, *Water Resources Research*, 49, 7644–7657, <https://doi.org/10.1002/2012WR013149>, 2013.
- Herbstritt, B., Gralher, B., and Weiler, M.: Continuous, near-real-time observations of water stable isotope ratios during rainfall and through-fall events, *Hydrology and Earth System Sciences*, 23, 3007–3019, 2019.
- Higham, D. J.: Condition numbers and their condition numbers, *Linear Algebra and its Applications*, 214, 193 – 213, [https://doi.org/https://doi.org/10.1016/0024-3795\(93\)00066-9](https://doi.org/https://doi.org/10.1016/0024-3795(93)00066-9), 1995.
- 600 Hinton, M. J., Schiff, S. L., and English, M. C.: Examining the contributions of glacial till water to storm runoff using two- and three-component hydrograph separations, *Water Resources Research*, 30, 983–993, <https://doi.org/10.1029/93WR03246>, 1994.
- Hoeg, S.: On the Balance Equations and Error Estimators for Separating n Time Components of Runoff With One Stable Isotope Tracer, *Water Resources Research*, 55, 8252–8269, <https://doi.org/10.1029/2019WR025555>, 2019.
- Hoeg, S., Uhlenbrook, S., and Leibundgut, C.: Hydrograph separation in a mountainous catchment — combining hydrochemical and isotopic  
 605 tracers, *Hydrological Processes*, 14, 1199–1216, [https://doi.org/10.1002/\(SICI\)1099-1085\(200005\)14:7<1199::AID-HYP35>3.0.CO;2-K](https://doi.org/10.1002/(SICI)1099-1085(200005)14:7<1199::AID-HYP35>3.0.CO;2-K), 2000.
- Hooper, R. P.: Diagnostic tools for mixing models of stream water chemistry, *Water Resources Research*, 39, <https://doi.org/10.1029/2002WR001528>, 2003.
- Hooper, R. P. and Shoemaker, C. A.: A Comparison of Chemical and Isotopic Hydrograph Separation, *Water Resources Research*, 22,  
 610 1444–1454, <https://doi.org/10.1029/WR022i010p01444>, 1986.
- Hrachowitz, M., Soulsby, C., Tetzlaff, D., Malcolm, I. A., and Schoups, G.: Gamma distribution models for transit time estimation in catchments: Physical interpretation of parameters and implications for time-variant transit time assessment, *Water Resources Research*, 46, <https://doi.org/10.1029/2010WR009148>, 2010.
- Iorgulescu, I., Beven, K. J., and Musy, A.: Flow, mixing, and displacement in using a data-based hydrochemical model to predict conservative  
 615 tracer data, *Water Resources Research*, 43, <https://doi.org/10.1029/2005WR004019>, 2007.
- James, A. and Roulet, N.: Antecedent moisture conditions and catchment morphology as controls on spatial patterns of runoff generation in small forest catchments, *Journal of Hydrology*, 377, 351 – 366, <https://doi.org/https://doi.org/10.1016/j.jhydrol.2009.08.039>, 2009.
- Jasechko, S.: Global Isotope Hydrogeology—Review, *Reviews of Geophysics*, 57, 835–965, 2019.
- Joerin, C., Beven, K., Iorgulescu, I., and Musy, A.: Uncertainty in hydrograph separations based on geochemical mixing models, *Journal of*  
 620 *Hydrology*, 255, 90 – 106, [https://doi.org/https://doi.org/10.1016/S0022-1694\(01\)00509-1](https://doi.org/https://doi.org/10.1016/S0022-1694(01)00509-1), 2002.
- Kendall, C. and McDonnell, J. J.: *Isotope Tracers in Catchment Hydrology*, Elsevier Science, Amsterdam, Netherlands, 1998.



- Kennedy, V., Kendall, C., Zellweger, G., Wyerman, T., and Avanzino, R.: Determination of the components of stormflow using water chemistry and environmental isotopes, Mattole River basin, California, *Journal of Hydrology*, 84, 107 – 140, [https://doi.org/https://doi.org/10.1016/0022-1694\(86\)90047-8](https://doi.org/https://doi.org/10.1016/0022-1694(86)90047-8), 1986.
- 625 Kirchner, J. W.: Aggregation in environmental systems – Part 2: Catchment mean transit times and young water fractions under hydrologic nonstationarity, *Hydrology and Earth System Sciences*, 20, 299–328, <https://doi.org/10.5194/hess-20-299-2016>, 2016.
- Kirchner, J. W.: Quantifying new water fractions and transit time distributions using ensemble hydrograph separation: theory and benchmark tests, *Hydrology and Earth System Sciences*, 23, 303–349, <https://doi.org/10.5194/hess-23-303-2019>, 2019.
- Kirchner, J. W. and Allen, S. T.: Seasonal partitioning of precipitation between streamflow and evapotranspiration, inferred from end-member  
630 splitting analysis, *Hydrology and Earth System Sciences*, 24, 17–39, <https://doi.org/10.5194/hess-24-17-2020>, 2020.
- Kirkby, M. J.: *Hillslope Hydrology*, John Wiley, Chichester, 1979.
- Klaus, J. and McDonnell, J.: Hydrograph separation using stable isotopes: Review and evaluation, *Journal of Hydrology*, 505, 47 – 64, <https://doi.org/https://doi.org/10.1016/j.jhydrol.2013.09.006>, 2013.
- Kuczera, G. and Parent, E.: Monte Carlo assessment of parameter uncertainty in conceptual catchment models: the Metropolis algorithm,  
635 *Journal of Hydrology*, 211, 69 – 85, [https://doi.org/https://doi.org/10.1016/S0022-1694\(98\)00198-X](https://doi.org/https://doi.org/10.1016/S0022-1694(98)00198-X), 1998.
- Ladouche, B., Probst, A., Viville, D., Idir, S., Baqué, D., Loubet, M., Probst, J.-L., and Bariac, T.: Hydrograph separation using isotopic, chemical and hydrological approaches (Strengbach catchment, France), *Journal of Hydrology*, 242, 255 – 274, [https://doi.org/https://doi.org/10.1016/S0022-1694\(00\)00391-7](https://doi.org/https://doi.org/10.1016/S0022-1694(00)00391-7), 2001.
- Laudon, H., Hemond, H. F., Krouse, R., and Bishop, K. H.: Oxygen 18 fractionation during snowmelt: Implications for spring flood hydro-  
640 graph separation, *Water Resources Research*, 38, 40–1–40–10, <https://doi.org/10.1029/2002WR001510>, 2002.
- Li, H. and Sivapalan, M.: Effect of spatial heterogeneity of runoff generation mechanisms on the scaling behavior of event runoff responses in a natural river basin, *Water Resources Research*, 47, <https://doi.org/10.1029/2010WR009712>, 2011.
- Lyon, S., L. E. Desilets, S., and Troch, P.: Characterizing the response of a catchment to an extreme rainfall event using hydrometric and isotopic data, *Water Resources Research - WATER RESOUR RES*, 44, <https://doi.org/10.1029/2007WR006259>, 2008.
- 645 Mallock, R. R. M. and Darwin, C. G.: An electrical calculating machine, *Proceedings of the Royal Society of London. Series A, Containing Papers of a Mathematical and Physical Character*, 140, 457–483, <https://doi.org/10.1098/rspa.1933.0081>, 1933.
- Maloszewski, P. and Zuber, A.: Determining the turnover time of groundwater systems with the aid of environmental tracers 1. Models and their applicability, *Journal of Hydrology*, 57, 207–231, [https://doi.org/10.1016/0022-1694\(82\)90147-0](https://doi.org/10.1016/0022-1694(82)90147-0), 1982.
- Martinec, J., Siegenthaler, U., Oeschger, H., and Tongiorgi, E.: New Insights into the Run-off Mechanism by Environmental Isotopes, in:  
650 *Symposium Isotope Techniques in Groundwater Hydrology*, vol. 38, pp. 143–157, International Atomic Energy Agency (IAEA), 1974.
- Matsubayashi, U., Velasquez, G. T., and Takagi, F.: Hydrograph separation and flow analysis by specific electrical conductance of water, *Journal of Hydrology*, 152, 179 – 199, 1993.
- Maulé, C. P. and Stein, J.: Hydrologic Flow Path Definition and Partitioning of Spring Meltwater, *Water Resources Research*, 26, 2959–2970, <https://doi.org/10.1029/WR026i012p02959>, 1990.
- 655 McDonnell, J. J., McGuire, K., Aggarwal, P., Beven, K. J., Biondi, D., Destouni, G., Dunn, S., James, A., Kirchner, J., Kraft, P., Lyon, S., Maloszewski, P., Newman, B., Pfister, L., Rinaldo, A., Rodhe, A., Sayama, T., Seibert, J., Solomon, K., Soulsby, C., Stewart, M., Tetzlaff, D., Tobin, C., Troch, P., Weiler, M., Western, A., Wörman, A., and Wrede, S.: How old is streamwater? Open questions in catchment transit time conceptualization, modelling and analysis, *Hydrological Processes*, 24, 1745–1754, <https://doi.org/10.1002/hyp.7796>, 2010.



- McGuire, K. J. and McDonnell, J. J.: A review and evaluation of catchment transit time modeling, *Journal of Hydrology*, 330, 543 – 563, 2006.
- Niemi, A. J.: Residence time distributions of variable flow processes, *The International Journal of Applied Radiation and Isotopes*, 28, 855–860, [https://doi.org/10.1016/0020-708X\(77\)90026-6](https://doi.org/10.1016/0020-708X(77)90026-6), 1977.
- Obradovic, M. M. and Sklash, M. G.: An isotopic and geochemical study of snowmelt runoff in a small arctic watershed, *Hydrological Processes*, 1, 15–30, <https://doi.org/10.1002/hyp.3360010104>, 1986.
- Ogunkoya, O. and Jenkins, A.: Analysis of storm hydrograph and flow pathways using a three-component hydrograph separation model, *Journal of Hydrology*, 142, 71 – 88, 1993.
- Pinder, G. F. and Jones, J. F.: Determination of the ground-water component of peak discharge from the chemistry of total runoff, *Water Resources Research*, 5, 438–445, <https://doi.org/10.1029/WR005i002p00438>, 1969.
- Rigon, R., Bancheri, M., and Green, T. R.: Age-ranked hydrological budgets and a travel time description of catchment hydrology, *Hydrology and Earth System Sciences*, 20, 4929–4947, <https://doi.org/10.5194/hess-20-4929-2016>, 2016.
- Rinaldo, A., Beven, K. J., Bertuzzo, E., Nicotina, L., Davies, J., Fiori, A., Russo, D., and Botter, G.: Catchment travel time distributions and water flow in soils, *Water Resources Research*, 47, <https://doi.org/10.1029/2011WR010478>, 2011.
- Saxena, R. K.: Estimation of Canopy Reservoir Capacity and Oxygen-18 Fractionation in Throughfall in a Pine Forest: Paper presented at the Nordic Hydrological Conference (Reykjavik, Iceland, August - 1986), *Hydrology Research*, 17, 251–260, <https://doi.org/10.2166/nh.1986.0017>, 1986.
- Schmieder, J., Garvelmann, J., Marke, T., and Strasser, U.: Spatio-temporal tracer variability in the glacier melt end-member — How does it affect hydrograph separation results?, *Hydrological Processes*, 32, 1828–1843, <https://doi.org/10.1002/hyp.11628>, 2018.
- Segura, C., James, A. L., Lazzati, D., and Roulet, N. T.: Scaling relationships for event water contributions and transit times in small-forested catchments in Eastern Quebec, *Water Resources Research*, 48, <https://doi.org/10.1029/2012WR011890>, 2012.
- Sklash, M. G. and Farvolden, R. N.: The role of groundwater in storm runoff, *Journal of Hydrology*, 43, 45–65, [https://doi.org/10.1016/0022-1694\(79\)90164-1](https://doi.org/10.1016/0022-1694(79)90164-1), 1979.
- Stoer, J.: *Numerische Mathematik 1*, Springer Lehrbuch, Springer Verlag Berlin Heidelberg New York, 1994.
- Turing, A. M.: ROUNDING-OFF ERRORS IN MATRIX PROCESSES, *The Quarterly Journal of Mechanics and Applied Mathematics*, 1, 287–308, <https://doi.org/10.1093/qjmam/1.1.287>, 1948.
- Uhlenbrook, S. and Hoeg, S.: Quantifying uncertainties in tracer-based hydrograph separations: a case study for two-, three- and five-component hydrograph separations in a mountainous catchment, *Hydrological Processes*, 17, 431–453, <https://doi.org/10.1002/hyp.1134>, 2003.
- Uhlenbrook, S., Frey, M., Leibundgut, C., and Maloszewski, P.: Hydrograph separations in a mesoscale mountainous basin at event and seasonal timescales, *Water Resources Research*, 38, 31–1–31–14, <https://doi.org/10.1029/2001WR000938>, 2002.
- Von Freyberg, J., Studer, B., Rinderer, M., and Kirchner, J. W.: Studying catchment storm response using event- and pre-event-water volumes as fractions of precipitation rather than discharge, *Hydrology and Earth System Sciences*, 22, 5847–5865, <https://doi.org/10.5194/hess-22-5847-2018>, 2018.
- Weiler, M., McGlynn, B. L., McGuire, K. J., and McDonnell, J. J.: How does rainfall become runoff? A combined tracer and runoff transfer function approach, *Water Resources Research*, 39, <https://doi.org/10.1029/2003WR002331>, 2003.
- Zoch, R. T.: On the relation between rainfall and stream flow, *Monthly Weather Review*, 62, 315–322, [https://doi.org/10.1175/1520-0493\(1934\)62<315:OTRBRA>2.0.CO;2](https://doi.org/10.1175/1520-0493(1934)62<315:OTRBRA>2.0.CO;2), 1934.